

5

MASS LOSS

Leo Goldberg

OVERVIEW

The first observational evidence for mass loss from cool stars was the discovery by Adams and MacCormack (1935) of blue-displaced components in low-excitation lines of metals in the spectra of certain red giant stars. The first systematic study of displaced lines was made by Deutsch (1956, 1960), who demonstrated that the matter forming the blue-shifted lines was actually escaping from the M-type component of the α Her system and that the phenomenon was common to all M giants and supergiants. Deutsch derived estimates of the mass loss for these stars, in the neighborhood of $10^{-7} M_{\odot}/\text{yr}$ —ten million times as great as the amount lost through the solar wind—and enough to affect the course of the late stages of stellar evolution in a major way.

Weymann (1962a) carried out a detailed spectrophotometric study of the spectrum of α Ori, the first real attempt at a quantitative analysis of the spectrum of the outflowing matter. He found that, despite variations of up to 10 km/s in the radial velocity of the photosphere, the displaced lines had not varied by as

much as 2 km/s over an interval of more than 20 years, which implied a detached shell far enough away to be uncoupled from the pulsation of the photosphere. He estimated the inner radius of the shell to be at least 14 stellar radii, from which the rate of mass loss was inferred to be $4.5 \times 10^{-6} M_{\odot}/\text{yr}$. Weymann (1962b) also demonstrated that the mass loss in α Ori could not be driven by thermal gas pressure, as it is in the solar corona.

After Weymann's work and following the development of more sensitive detectors, interest shifted to the infrared region of the spectrum. Red giants were found to emit an excess of infrared radiation, as compared with a blackbody, in a broad band of wavelengths centered at about 9.7 μm . Woolf and Ney (1969) attributed the emission to dust grains in an extensive circumstellar shell and suggested that the grains were made of silicates containing metallic impurities such as Fe, Mg, and Al (e.g., MgSiO_3 and olivine, $(\text{Mg,Fe})_2\text{SiO}_4$). From calculations of chemical equilibrium, Gilman (1969) showed that such molecules can condense in cool atmospheres of oxygen-rich stars (K and M stars) and identified similar

emissions at 11 μm as condensates of C in carbon-rich stars (R and N stars) and of SiC in stars with equal abundances of carbon and oxygen (S stars). Hoyle and Wickramasinghe (1962) had suggested earlier that graphite grains would condense in the outer regions of C-rich stellar atmospheres with sufficiently low temperatures. Gehrz and Woolf (1971) supposed that radiation pressure on the dust grains would propel them away from the star, dragging the gas along with it, and, using observed color excesses at 11 μm to estimate rates of mass loss for more than 50 stars, they derived values in the range 5×10^{-8} to $3 \times 10^{-5} M_{\odot}/\text{yr}$. There was still serious doubt as to whether the momentum acquired by the grains could be transmitted to the gas, in view of the very long mean free path for grain-gas collisions (Weymann, 1962b) until Gilman (1972) showed that the gas and dust are momentum-coupled and not position-coupled (i.e., primary collisions transmit momentum from dust to gas, but secondary collisions between atoms (molecules) are the principal means by which momentum is distributed through the gas). The process was shown to work for both silicate and graphite grains.

The large values of mass loss inferred from the dust emission heightened interest in mass loss from red giants as an important factor in the late stages of stellar evolution and as a major source both of the enrichment of interstellar gas by heavy elements and of the interstellar dust itself. As one result, Reimers (1975a, 1975b) undertook a systematic program of analysis of circumstellar absorption lines in the optical spectra of more than 120 K and M giants and G, K, and M supergiants. In these and later papers (see Reimers, 1981), Reimers found that the stars showing circumstellar absorption lines in their spectra, as evidence of high rates of mass loss, were confined to the upper right-hand corner of the Hertzsprung-Russell (HR) diagram and that terminal flow velocities ranged from about 5 to over 100 km/s. The wind velocity was found to increase roughly as the square of the escape velocity

from the photosphere. Except in a few cases, Reimers did not publish mass-loss rates derived for individual stars, but instead presented his results in the form of an interpolation formula:

$$\dot{M} = 4 \times 10^{-13} L/gR (M_{\odot}/\text{yr}) \quad , \quad (5-1)$$

where L is the star's luminosity, R is its radius, and g is the acceleration of gravity, all in solar units. This equation was derived from dimensional considerations, its physical significance being that the kinetic energy required to carry the escaping mass from a star to infinity is always the same fraction of the star's luminosity. The constant was evaluated by the process of fitting the formula to 4 or 5 normal points derived from the empirical mass-loss rates. Because of uncertainties in the empirical rates, as well as in L , M , and R , the proportionality constant is generally believed to be accurate only within a factor of 10. Reimers' formula has been the principal source of information on empirical rates of mass loss from red giants used in theoretical calculations of stellar evolution.

More refined methods of analysis were applied to a relatively small number of selected stars by Sanner (1976), Bernat (1977), and Hagen (1978). Hagen attempted to derive separate rates of mass loss for both the gas (from the optical lines) and the dust (from the 10- μm emission feature). The absence of reasonable agreement among the rates derived by these investigators made it apparent that far too little is known about the structure and composition of red giant atmospheres, as will become evident further on.

Observations with the International Ultraviolet Explorer (IUE) and with the High Energy Astrophysical Observatory (HEAO) have illuminated further the nature of the division in the HR diagram between stars with high and low rates of mass loss. The short-wavelength limit of observation with IUE is about 1170 \AA , which reaches lines formed in the chromosphere/corona transition region, but not the coronal lines themselves. What at first appeared to be a

sharp line dividing stars with hot coronas from those with cool massive winds (Linsky and Haisch, 1979) is now seen as a gradual transition, with some stars in the boundary zone showing both types of spectra (Hartmann et al., 1980; see also Dupree, 1980; Reimers, 1981). Stars near the boundary tend to show temporal variations in the mass flows.

New techniques for observing at infrared, millimeter, and centimeter wavelengths are currently leading to dramatic advances in knowledge of the rates and evolutionary implications of mass loss from highly evolved stars. Observations with very high resolution of the vibration/rotation line spectra of CO, including both fundamental and overtone bands, have been effective in probing the structures of mass flows from red giants, especially Miras (Hall, 1980). Emission from circumstellar shells in the 1-0 and 2-1 transitions of CO at millimeter wavelengths can give direct information on stellar velocities, shell expansion velocities, shell sizes, and, with appropriate modeling, estimates of mass loss (Knapp et al., 1982; Knapp and Morris, 1984). Flux densities of radio continuum radiation measured with the very large array (VLA) may now be used to infer the temperature and extent of chromospheres in red giants. The VLA has also been used to map the α Sco system (Hjellming and Newell, 1983), in which the creation of an H II region in the expanding shell of the M star by the ultraviolet (UV) radiation of the B star permits a determination of the rate of mass loss from the M star. Finally, maser radiation emitted by H₂O, SiO, and OH has been shown in principle to yield information on the structure of various regions of late-type atmospheres and on the enormous extent of their circumstellar shells (see Elitzur, 1981). The so-called OH/IR stars offer the possibility of studying very luminous, long-period Mira variables which are not seen in visible light.

The observational study of mass loss from red giants in globular clusters was initiated by Cohen (1976), who interpreted emission associated with the H α absorption line as arising by recombination in an expanding ionized shell of hydrogen. The same method has been ex-

tended to large numbers of stars by Mallia and Pagel (1978), Peterson (1981, 1982), and especially by Cacciari and Freeman (1981, 1983), all of whom derived rates in the neighborhood of $10^{-8} M_{\odot}/\text{yr}$. Although rates of this order of magnitude seem to satisfy the requirements of stellar evolution, there is a fundamental difficulty in the assumption that the presence of H α emission is by itself evidence of mass loss (Reimers, 1981; Dupree, et al, 1984).

In addition to thermal gas pressure and radiation pressure on dust grains, a number of other interesting mechanisms have been proposed for both steady and episodic mass loss (e.g., wave pressure, shock waves, magnetic reconnection, dynamical and pulsational instability, and pulsational mode switching in Miras). The probability is high that the dust mechanism operates in the coolest late-type stars, but it is not at all clear which mechanisms are most relevant in other stars.

Mass loss from red giants plays a crucial role in several aspects of stellar evolution (see Renzini, 1981a; Iben, 1981b). Mass loss from stars of intermediate mass between 1 and $8 M_{\odot}$ can make an important contribution to the enrichment of the interstellar medium. Moreover, in the absence of mass loss, all stars with masses exceeding $1.4 M_{\odot}$ would become supernovae, but if enough mass is lost while the star is on the asymptotic giant branch (AGB) of the HR diagram, intermediate-mass stars may evolve into planetary nebulae and white dwarfs. Particularly exciting is the recognition of long-period OH/IR stars as possible progenitors of planetary nebulae. Mass loss from intermediate-mass stars may also affect the formation of interstellar dust grains, Mira variables, and carbon stars. The evolution of low-mass stars (mass less than $1.4 M_{\odot}$) has been extensively studied in globular clusters. In the absence of mass loss, one finds discrepancies between the observed and calculated luminosity functions of stars on the horizontal branch (HB) and AGB, which can be removed by postulating mass losses of about $0.2 M_{\odot}$ on the red-giant branch (RGB) and about $0.1 M_{\odot}$ on the AGB.

EMPIRICAL RATE DETERMINATIONS

UV-Optical Spectra 0.2–5 μm

Single Stars. Figure 5-1 shows small regions of the spectra of several red giants and supergiants centered on the resonance lines of Mg + , Ca + , Na, Mn, and K. The profiles are more or less typical of the resonance lines of neutral and singly ionized metals in the visible and near-UV spectral regions of cool stars showing mass loss. Figure 5-2 shows a tracing of the R1 line of the 1–0 band of CO near 4.65 μm , which is similar in appearance to the potassium line. The cores of the Mg II and Ca II lines are strongly saturated and contaminated by chromospheric emission, but the other lines show the P Cygni profiles characteristic of resonance scattering in an extended expanding atmosphere, although distorted by the underlying, broad photospheric line. The absorption components are formed along the line of sight to the star and are displaced to the blue by the amount of the expansion velocity, whereas the emission is undisplaced relative to the center-of-mass velocity. Notice that in α Ori, the CO and K I circumstellar (CS) lines are double, with an apparent separation of about 6.5 km/s, implying the existence of two discrete shells. Curiously, in this star, the doubling is also seen in the D-lines of Na I, but not in any other lines. The absence of shell components among lines with excitation potentials greater than a few tenths of a volt has been interpreted as implying shell temperatures less than 1000 K (Weymann, 1962a).

Spectral line profiles are used for the derivation of mass-loss rates with the aid of the equation of continuity:

$$\dot{M} = 4\pi \cdot r^2 \cdot n(r) \cdot \mu \cdot m_H \cdot v(r) , \quad (5-2)$$

where r is the radius of a volume element with hydrogen number density $n(r)$ and outward

velocity $v(r)$, μ is the mean molecular weight, and m_H is the mass of the H atom. This equation implies steady mass loss with spherical symmetry. In most cases, the radial dependence of velocity and density cannot be determined without additional assumptions. Since the circumstellar absorption lines appear to be relatively sharp, the velocity along the line of sight is usually assumed to be constant, which implies an inverse square law for the density. Moreover, the formation of P Cygni profiles signifies that most of the emission is occurring far from the star, and the radial velocities of the displaced components are constant even in stars with variable photospheric velocities. Therefore, the circumstellar shells are assumed to be detached from the stellar photospheres and to be far enough away to be insensible to their motions. With these two assumptions, Equation (5-2) becomes:

$$\dot{M} = 4\pi \cdot N \cdot \mu \cdot m_H \cdot R_o \cdot V , \quad (5-3)$$

where N is the column density of hydrogen gas along the line of sight, R_o is the inner radius of the detached shell, and V is the expansion velocity, assumed to be constant. The derivation of \dot{M} from Equation (5-3) proceeds by steps as follows.

First, the P Cygni profile must be detached from the background photospheric line, which can be done with varying degrees of difficulty. Two quantities are extracted from the line profile: the column density of atoms or molecules in the ground level of a particular transition and the expansion velocity. The earlier work (Weymann, 1962a; Reimers, 1975a) assumed line formation in a static, plane-parallel atmosphere, but more recent work has made use of relatively exact calculations by Kunasz and Hummer (1974) of radiative transfer in an expanding spherical atmosphere and of relatively sophisticated non-LTE calculations of ionization equilibrium (Sanner, 1976; Bernat, 1977; Hagen, 1978). On the average, column densities derived by Bernat (1977) for α Ori are smaller

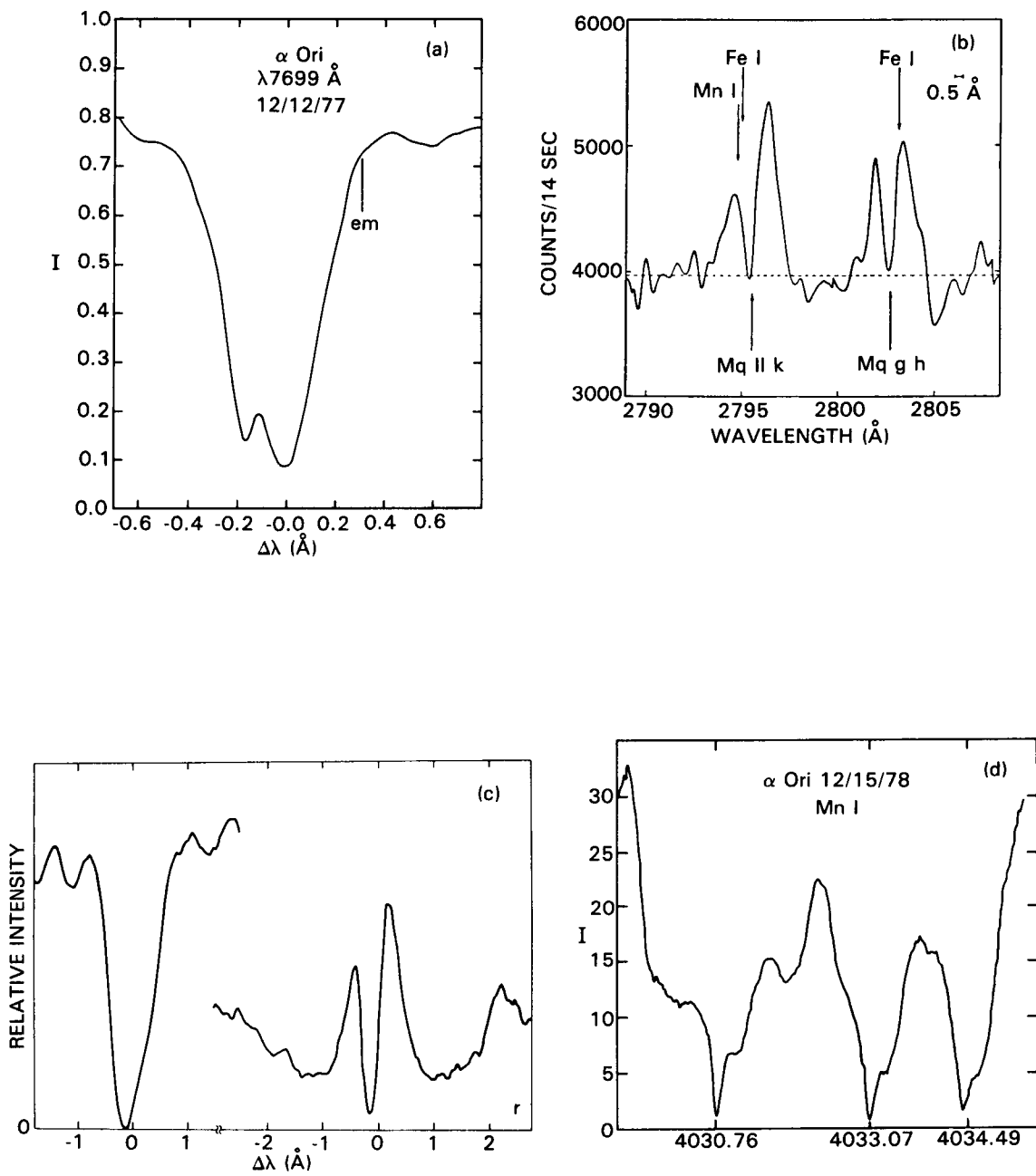


Figure 5-1. Circumstellar resonance line profiles: (a) K I in Ori; (b) Mg II in α Ori (Bernat 1976); (c) Na I 5890 \AA in α Her (left); Ca II K in β Peg (Hagen, 1980) (right); (d) Mn I in α Ori. The vertical line labeled "em" in (a) marks the center of the emission component of the P Cygni profile.

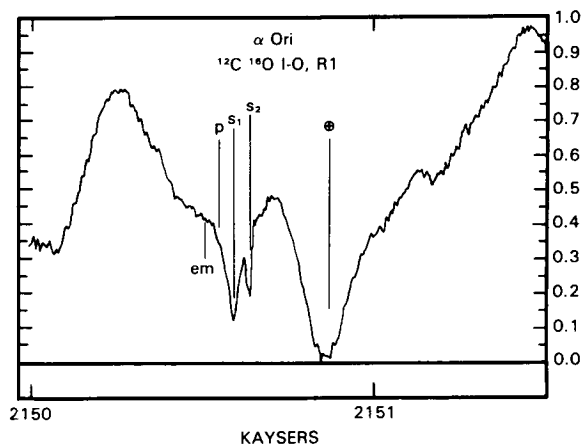


Figure 5-2. The R1 line of the 1-0 band of CO in the spectrum of α Ori. The two shell components, s_1 and s_2 , are superposed on the broad photospheric line labeled p . The strong telluric component is shown to the right (Bernat et al., 1979). The vertical line labeled "em" marks the center of the emission component of the P Cygni profile.

than those of Weymann (1962a) by a factor of 3 to 4. The expansion velocity, V , is obtained by direct measurement of the displacement of the absorption line relative to neighboring photospheric lines. The emission on the redward side of the absorption line causes a spurious additional shift of the line, amounting to an error of about 25 percent (Bernat, 1976). If the velocity of the photosphere is variable, the expansion velocity is the shell velocity minus the center-of-mass velocity.

The column density of the given atom in a given stage of ionization must then be converted into, first, the column density of the element in all stages of ionization and, second, the column density of hydrogen. Most of the resonance lines seen in the visible spectrum, with the exception of those of Ca II, Sr II, and Ba II, belong to neutral metals such as Fe, Cr, Ni, Mn, and K. Since the metals are predominantly singly ionized, a theory of ionization is needed to derive the abundance of the ion. This step is omitted for Sr II and Ba II. The total column density then follows from the assumption

that the abundances are solar-like, which may be reasonable for most of the metals but is questionable for Sr and Ba. The assumptions made for CO in O-rich stars are that all carbon atoms are locked up in CO, which seems reasonable, and that the C/H ratio is the same as in the Sun, which is a pure guess.

Applications of the theory of ionization have led to severe contradictions in the results. As a test of the theory, Hagen (1978) derived column densities of Sr II and Ba II in eight stars and then used solar abundances and ionization theory to predict column densities for several neutral metals. Figure 5-3 shows the logarithm of the ratio of the observed column density $N(\text{obs})$ to the predicted column density $N(\text{pred})$ plotted against the element in order of decreasing ionization potential. The discrepancy of four orders of magnitude is hard to explain. Part of it apparently results from the steep drop of the assumed blackbody radiation field below 2000 Å, and part may be caused by the depletion in grains of elements with higher ionization potentials. Figure 5-3 suggests that neutral elements of low ionization potential are much more abundant than the theory predicts and raises a question as to whether Ba and Sr are indeed predominantly singly ionized, at least in the cooler M giants.

Hagen (1978) used only the lines of Sc II, Sr II, and Ba II to derive column densities of hydrogen in eight red giants. Bernat (1977) derived hydrogen column densities in the four red supergiants— α Ori, α Sco, α Her, and μ Cep—by averaging the results obtained from 8 to 9 metallic atoms, both neutral and singly ionized. Although the scatter is large, approaching a factor of 50, there is no systematic difference between hydrogen column densities derived from neutral and ionized species, respectively. On the other hand, the column densities inferred from the Ti II lines at 3300 Å are too small relative to those from Sr II and Ba II by factors of 7 to 20, if solar relative abundances are used and if the singly ionized stage is assumed to be predominant.

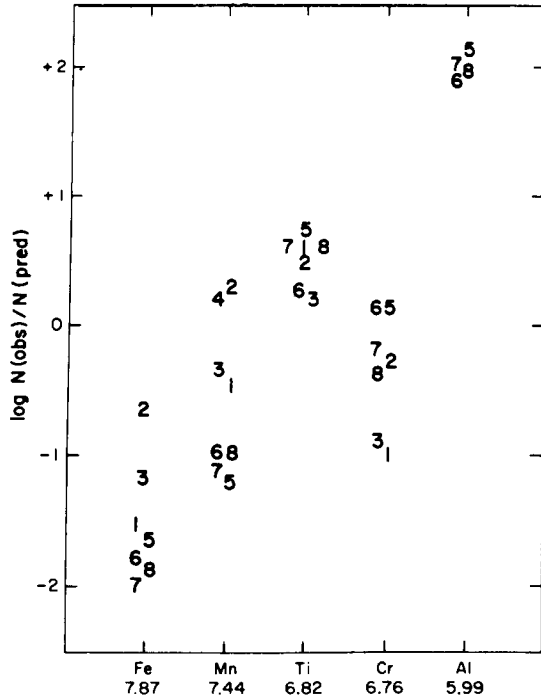


Figure 5-3. The logarithm of the ratio of the observed column density of neutral atoms to the column density predicted through the use of ionization theory and solar abundances plotted against element in order of decreasing ionization potential. The numbers refer to different stars as follows: 1 = *X Her*, 2 = *RX Boo*, 3 = *HD 207076*, 4 = *R Leo*, 5 = *α Sco*, 6 = *α Ori*, 7 = *α Her*, 8 = *μ Cep* (Hagen, 1978).

A very large error in \dot{M} may arise because there is often no satisfactory method available for the determination of R_o , the inner radius of the shell; different investigators have used values differing by one or two orders of magnitude for the same star. Weymann (1962a) proposed a method for deriving the inner radius based on the idea that the cores of the infrared triplet lines of Ca II, 8542 and 8662 Å, might show small displaced absorption components formed in the expanding shell. Since the lower levels of these lines should be populated by radiative excitation, the equivalent width of the feature ought to be inversely related to the shell radius. The method has been applied to several

stars by Weymann (1962a), Sanner (1976), and Bernat (1977), and although it appears to work in some stars, it leads to widely discrepant results for *α Ori*, for which the lines are so deep that the signal to noise tends to be relatively small at the very line center (Goldberg, 1979). Another method of estimating R_o is based on model calculations of off-limb profiles of K I emission (Bernat, 1976). When the line of sight is interior to the inner radius, the calculated profiles are asymmetric, and the observation of such asymmetries in Betelgeuse implies an inner radius of about 100 stellar radii, but the calculations are strongly model-dependent.

There is in fact some question as to whether the shell has a well-defined inner radius, as is usually assumed in mass-loss determinations. No matter what the mechanism for initiating and maintaining the flow may be, there must be a region in which the gas accelerates to its terminal velocity and in which the density is relatively high. Such a region would be difficult to identify from a P Cygni profile because, although the absorption component might be strongly asymmetrical, the asymmetry would be camouflaged by the redward-shifted emission component. The superposition of a P Cygni profile on a photospheric line would make such an asymmetry doubly difficult to detect. On the other hand, subordinate lines would not be expected to display strong redward emission, since photons absorbed in such lines tend to be re-emitted in resonance lines. Such asymmetric subordinate lines are indeed observed in the spectrum of *α Ori*, the most prominent among them being the Fe I lines at 4140 Å and the Ca II IR triplet (Goldberg, 1979), both of which have excitation potentials of about 1.5 eV. The 8498 and 8542 Å lines of Ca II are shown in Figure 5-4, where they are plotted on a heliocentric velocity scale. Notice that the line cores are highly asymmetric in the sense that the radial velocity decreases from about 21 to 22 km/s, which is the systemic velocity of the star, in the upper part of the core, to about 13.5 km/s at the bottom of the 8542 Å line. Moreover, over a period of several years, during

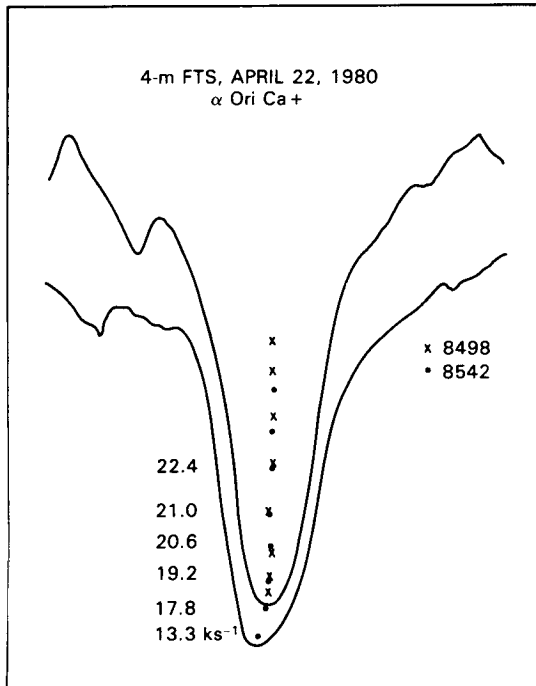


Figure 5-4. Profiles of the 8498 and 8542 Å lines of Ca II in α Ori made with the Fourier transform spectrometer of the McMath Telescope at Kitt Peak National Observatory. The lines are plotted on a velocity scale. The line bisectors are indicated by dots (8498 Å) and crosses (8542 Å), with the corresponding heliocentric velocities shown to the left.

which the mean velocity of the photosphere decreased by about 5 km/s, the velocities in these profiles remained stationary (Goldberg, 1979). The terminal velocity shown by the absorption components of the resonance lines is about 11 km/s, but if a correction is made for the spurious shift caused by their companion emission lines, the velocity would agree with that measured at the center of the 8542 Å line. Thus, the line is formed in an atmospheric region which is far enough away to be uncoupled from the motion of the photosphere, which is an argument in favor of the detached shell model. It is probable that the absorption components of the resonance lines would show the same behavior if they could be separated from their emission components.

The first high-resolution observations of circumstellar CO were made in the spectrum of α Ori by Bernat et al. (1979) with the Fourier transform spectrometer (FTS) at the Kitt Peak National Observatory (KPNO) 4-meter telescope. Numerous lines of the fundamental vibration/rotation band at 4.6 μm were observed, including several lines of the isotopic molecule, ^{13}CO . Subsequently, Bernat (1981) observed the band in nine other red giants. Figure 5-2 shows a typical CO line in the spectrum of Betelgeuse, which consists of four components: a telluric line, a broad photospheric line, and two narrow circumstellar lines with heliocentric velocities of 11.0 and 4.8 km/s, respectively. The same velocity components are observed in K I and probably also in the D-lines of Na (Goldberg et al., 1975), but in no other lines. The relative abundances $^{12}\text{C}/^{13}\text{C}$ were found to be about 6 for both components, which suggests two shells with a common origin in highly processed matter from the stellar interior and thus rules out an interstellar origin for the second component. After showing that collisional excitation dominates over radiative excitation, Bernat et al. (1979) identify the excitation temperature with the kinetic temperature, assume that the gas and dust are in thermal equilibrium, and derive distances of 150 and 2000 stellar radii, respectively, for the two shells. The further assumptions of cosmic composition and the complete association of carbon into CO lead to mass-loss rates of 5×10^{-6} and $3.2 \times 10^{-6} M_{\odot}/\text{yr}$ for the near and far shells, respectively.

The results of Bernat's (1981) survey of other red giants for circumstellar CO are shown in Table 5-1. In addition to these stars, three other stars— α Boo, α Tau, and α Sco—showed no detectable CO, whereas the CO shell lines in RX Boo were found to be too strongly saturated for analysis. α Boo and α Tau are too early in spectral type to show circumstellar lines, and as Bernat points out, any CO in the shell of α Sco would be dissociated by the companion B star. Table 5-1 shows that the CO absorption features are multiple in many stars,

Table 5-1
Observations of CO in M Giants and Supergiants (Bernat, 1981)

Star	Spectral Type	Component (km/s)	T_{exc} (K)	$N(\text{CO})/v$ (Dop) (cm ⁻² km ⁻¹ s)	$N(\text{H})$ (cm ⁻²)	$N(\text{Dust})^a$ (cm ⁻²)
119 Tau	M2 Iab-Ib	-9	200 ± 150	7.5 + 15	3.4 + 21 ^b	—
μ Cep	M2 Ia	-8	100 ± 10	7.5 + 15	7.3 + 21 ^c	—
		-13	270 ± 60	2.0 + 16	—	—
		-19	100 ± 15	1.8 + 16	—	4.0 + 21 ^d
		-38	60 ± 4	1.1 + 17	—	—
		-47	100 ± 40	3.0 + 15	—	—
β Peg	M2-3II-III	-6	90 ± 30	1.3 + 16	2.7 + 20 ^b	—
ρ Per	M4 II-III	-2	90 ± 20	6.5 + 15	2.7 + 20 ^b	—
α Her	M5 Ib-II+	-13	250 ± 60	4.2 + 16	6.6 + 21 ^d	2.0 + 20 ^d
		-25	550 ± 670	6.7 + 15	—	—
SW Vir	M7 III	-6	130 ± 20	2.9 + 16	—	—
		-9	130 ± 15	2.3 + 16	—	—
X Her	M6e	-8	110 ± 20	4.3 + 16	2.5 + 20 ^d	4.0 + 21 ^d
W Hya	M7-9e	-5	300 ± 90	4.8 + 16	2.5 + 20 ^d	6.0 + 21 ^d
		-13	120 ± 20	3.7 + 15	—	—

^a $N(\text{Dust})$ is the H column density derived assuming cosmic abundances and complete condensation of silicates.

^bSanner (1976).

^cBernat (1977).

^dHagen (1978).

which Bernat now attributes to episodic mass loss rather than to the formation of discrete clumps by instabilities in a steady flow as was postulated for Betelgeuse (Bernat et al., 1979). Column 4 lists the excitation temperatures, interpreted as kinetic temperatures. The Doppler velocity could not be independently determined and therefore only the ratio of CO column density to Doppler velocity can be inferred, as given in column 5. Column 6 contains the hydrogen column densities derived in previous investigations of optical atomic spectra, and column 7 lists the hydrogen column density derived from the 10- μm silicate feature on the assumption that all Si atoms are condensed on grains and that the Si/H ratio has the solar value. The absence of a correlation between CO column densities and either of the two hydrogen column densities is, in Bernat's view, a major argument in favor of episodic mass loss, since the separate shells would be formed under different physical conditions.

Bernat's final conclusion is that meaningful mass-loss rates cannot be determined from observations of nonsteady mass loss unless averages are taken over several episodes. We shall come back later to the topic of episodic mass loss and comment here only that the absence of correlations between the various column densities is not unexpected in view of: (1) the large scatter of the determinations from different ions in the same star, and (2) the many sources of error in the derivation of column densities from the 10- μm emission feature.

Binary Stars. The errors introduced by uncertain knowledge of the degree of ionization and of the inner shell radius may be avoided in principle by observing circumstellar lines of elements in a predominant stage of ionization (e.g., Fe II or Ti II) in the spectrum of a hot visual companion of a red giant (Reimers, 1981). If the geometry of the binary system is known, no assumption need be made about an

inner shell radius. Stars studied in this way from the ground, from a balloon, and from IUE are α^1 Her (Reimers, 1977a) and α Sco A (Kudritzki and Reimers, 1978; van der Hucht et al., 1980; Bernat, 1982). Reimers (1977a) derived hydrogen column densities from six shell lines of Sr II (4077 Å) and Ti II (3300 Å) in the spectrum of α^2 Her (G5 III), the visual companion of α^1 Her (M5 II), and obtained a mass-loss rate of $1.1 \times 10^{-7} M_{\odot}/\text{yr}$, which is about one-sixth of Bernat's (1977) value derived from lines of neutral metals at visible wavelengths in the spectrum of α^1 Her.

The binary-star approach has been extensively applied to the α Sco system. Kudritzki and Reimers (1978) derived a rate of $7 \times 10^{-7} M_{\odot}/\text{yr}$ for mass loss from α Sco A (M1.5 Iab), using the H and K lines of Ca II and the Ti II lines in the spectrum of α Sco B (B2.5 II). Van der Hucht et al. (1980) observed a variety of lines between 2000 and 3000 Å in the spectrum of α Sco B with the balloon-borne ultraviolet spectrometer (BUSS), giving greatest weight to the Zn II and Cr II lines, and obtained a rate equal to $7.1 \times 10^{-6} M_{\odot}/\text{yr}$. It is possible that the Zn II lines are primarily interstellar (Reimers, 1981). Finally, Bernat (1982) has made the most thorough investigation of mass loss from α Sco A, with the IUE satellite, by observing 90 lines of about a dozen ions in the wavelength range 1190 to 2631 Å. The result is that the column densities of hydrogen, derived from 10 different ions, predominantly singly ionized, show a spread of a factor of 30. No single explanation—observational error, shell chemistry, interstellar contributions—appears to be satisfactory. An unweighted mean over all ions gives a rate of $6.4 \times 10^{-6} M_{\odot}/\text{yr}$.

In principle, the binary-star approach may be extended to a much larger number of stars by IUE observations of spectroscopic binaries consisting of a red-giant star and a B-type companion. Observations in the ultraviolet effectively separate the two stars. The first attempts along these lines were made for 32 Cyg (Stencel et al., 1979) and ζ Aur (Chapman, 1981), but

neglected to take into account the nonspherical nature of the line-transfer problem (Reimers, 1981). The angular separation of such objects is so small that radiation from both the B star and the circumstellar shell pass through the spectrograph slit, resulting in P Cygni profiles that must be analyzed in the context of a nonspherical three-dimensional line-transfer problem. The necessary theoretical framework has been developed by Hempe (1982) and applied to the analysis of a number of objects, including ζ Aur, 32 Cyg, and 31 Cyg (Che et al., 1983), δ Sge (Reimers and Schröder, 1983), and Boss 1985 (Che and Reimers, 1983). For the K supergiant, ζ Aur, Che et al. (1983) derived $\dot{M} = 0.63 \times 10^{-8} M_{\odot}/\text{yr}$ and $v_{exp} = 40$ km/s, as compared with Chapman's (1981) values of $\dot{M} = 2 \times 10^{-8} M_{\odot}/\text{yr}$ and $v_{exp} = 100$ km/s, respectively. For 32 Cyg, Che et al. found $\dot{M} = 2 \times 10^{-8} M_{\odot}/\text{yr}$ and $v_{exp} = 60$ km/s, as compared with Stencel et al.'s (1979) $4 \times 10^{-7} M_{\odot}/\text{yr}$ and 65 km/s, respectively.

Mira Stars. Optical studies of mass loss from Mira stars have benefited greatly from observations of the infrared vibration/rotation bands of CO. The star χ Cyg is a good example, in which a series of high-resolution spectra, taken with the FTS at the KPNO 4-meter telescope may have provided new insights into the mass-loss mechanism for red-giant stars (Hinkle et al., 1982). The spectra covered more than three cycles of the visible light variation and included the first and second overtone bands as well as the fundamental. Analysis has revealed four sets of lines, separated according to their velocity characteristics, and apparently arising from four different atmospheric regions: (1) a pulsating photospheric region through which a shock front passes near maximum light; (2) a cool gas ($T \sim 300$ K) expanding at 7.5 km/s relative to the center of mass, which is identified with the circumstellar shell; (3) a hotter region ($T \sim 800$ K), stationary with respect to the center of mass; and (4) a still hotter gas ($T \sim 1500$ K) falling inward at 8 km/s. The column density of the stationary layer varies on a time scale larger than the optical period of 410 days.

For example, the lines were absent in 1975, became quite pronounced 7 months later, and then weakened steadily over the next 3 years. It is conjectured that this layer contains gas ejected during particularly violent oscillations and is somehow supported by dissipated shock energy. If the stationary layer is heated by stellar photospheric radiation, its 800 K temperature implies a distance of $10 R_*$, or 1.7×10^{14} cm, where dust grains can form. Roughly the same value, 10^{14} cm, was measured by infrared speckle imaging techniques (Mariotti et al., 1983). Thus, it can provide a reservoir both for the dust-driven mass loss and the infalling gas. A similar layer appears to be present in the 10 Miras which have been observed thus far by Hinkle et al. (1982), who suggest that it may also be present in most late-type stars.

Red Giants in Globular Clusters. It has been known for some time (for a summary, see Renzini, 1981a) that a mass loss of about $0.2 M_\odot$ during the RGB (red-giant branch) phase, and an additional $0.1 M_\odot$ during the AGB (asymptotic giant branch) phase are needed to bring the calculated distribution of stars on the HR diagrams of globular clusters into agreement with observations. In the absence of experimental evidence for mass loss from stars in globular clusters, theorists incorporated into their calculations (Fusi-Pecci and Renzini, 1976; Renzini, 1977) Reimers' (1975a, 1975b) parametric formula for mass loss, Equation (5-2), modified by an adjustable parameter, η , which is supposed to reflect the uncertainty in the empirical rates:

$$\dot{M} = -4 \times 10^{-13} \times \eta \cdot L/gR. \quad (5-4)$$

This relationship was derived for Population I stars, and the scatter around it suggests that η lies somewhere between 0.3 and 3.0. It is therefore remarkable that, within rather close limits, the Reimers formula with $\eta = 0.40$ clears up both the HB and AGB discrepancies, despite the fact that it is based on empirical

rates for relatively few Population I stars, which are themselves uncertain by a factor of 10.

Observational evidence for mass loss from red giants in globular clusters was first offered by Cohen (1976) in the form of emission associated with the $H\alpha$ absorption lines in four red giants belonging to three globular clusters. Although emission has been observed on the blue wing in some cases, it has also been seen only on the red wing in other stars and on both wings in still others. Cohen's observations have been extended to a large number of stars in more than a dozen clusters by Mallia and Pagel (1978), by Peterson (1981, 1982), and especially by Cacciari and Freeman (1983). Cohen (1976) postulated that the emission arises from a circumstellar shell as a result of mass loss. As a model for estimating mass loss, Cohen took a completely ionized shell, expanding at a constant rate of 45 km/s from an inner shell radius $R_s = 2 R_*$ to infinity. The envelope was assumed to be optically thick in the Lyman lines and optically thin in the Balmer lines. With these assumptions, the total $H\alpha$ emission from the star is written as:

$$E(H\alpha) = 4\pi \cdot h\nu \cdot n_o^2 \cdot \alpha_{32} R_s^4 \int_{R_s}^{\infty} dr/r^2, \quad (5-5)$$

in ergs/s, where n_o is the density of hydrogen at R_s , and α_{32} is the effective recombination coefficient for a temperature of 10000 K.

The rate of mass loss is then

$$\dot{M} = 4\pi \cdot R_s^2 \cdot m_H \cdot V_{exp} \cdot n_o, \quad (5-6)$$

where n_o is to be substituted from Equation (5-5), and m_H is the mass of the hydrogen atom. Numerically, with the equivalent width W substituted for $E(H\alpha)$, the rate of mass loss becomes (Mallia and Pagel, 1978):

$$\dot{M} = 2.76 \times 10^{-4} V_{exp} \cdot R_* (R_s \cdot W)^{1/2} \cdot \exp(-1.1/T_4) \quad (5-7)$$

The radii are expressed in solar radii, V^{exp} is in km/s, W is in Å, T is in units of 10^4 K, and \dot{M} is in M_{\odot}/yr . Note that, when expressed in terms of the observed quantity, W , the equivalent width, \dot{M} , is proportional to $R_{*}^{3/2}$, and not to $R_{*}^{1/2}$ as Cohen (1976) supposed.

All investigators have followed Cohen's (1976) methodology in calculating rates of mass loss. Cohen derived a minimum rate of $2 \times 10^{-9} M_{\odot}/\text{yr}$, which, when combined with a red-giant lifetime of 1×10^8 years, gave the desired loss of $0.2 M_{\odot}$ on the RGB. Mallia and Pagel (1978) found much larger rates, up to $6 \times 10^{-8} M_{\odot}/\text{yr}$, principally because they used larger stellar radii, but they also believed that their results were compatible with the requirements of HB morphology. In her study of seven luminous giants in three clusters, using high spectral resolution, Peterson (1981) found that the Na D and H α lines in some stars had blue-shifted asymmetric cores similar to those observed in M field giants and supergiants (Boesgaard and Hagen, 1979). The shifts amounted to about 6 km/s in H α and 11 km/s in Na D. Peterson (1981) notes that emission is not usually seen in field giants with asymmetric cores. Boesgaard and Hagen (1979) find that 50 percent of stars with spectral classes M0 III to M7 III show asymmetric H α profiles with core blue shifts of a few km/s.

In a recent extensive survey of 143 red giants in 12 globular clusters, Cacciari and Freeman (1983) detected H α emission in about one-third of the stars brighter than $\log L = 2.9$, or $M_{bol} < -2.5$, with clear evidence of variability. Moreover, the apparent narrowing of H α absorption in fainter stars suggests the presence of weaker emission down to $\log L = 2.3$, or $M_{bol} = -1$. Mass-loss rates calculated from Equation (5-7) are between 0.7 and 6.3 in units of $10^{-8} M_{\odot}/\text{yr}$. The required total mass loss on the RGB is attained if it is assumed that the average rate of loss from $M_{bol} = -1$ to the tip of the RGB is $10^{-8} M_{\odot}/\text{yr}$ over an evolutionary time of 2×10^7 years (Sweigart and Gross, 1978).

Despite these estimates, however, the occurrence of mass loss in globular cluster stars on

the RGB in an amount sufficient to satisfy evolutionary requirements is still unproven (Reimers, 1981; Dupree et al., 1984). Neither H α emission nor the dependence of the emission on luminosity is evidence of mass loss. Model calculations of H α line profiles in metal-deficient stars by Dupree et al. (1984) show that emission wings can arise in warm chromospheres with mass-loss rates $\ll 2 \times 10^{-9} M_{\odot}/\text{yr}$. Moreover, chromospheric activity might well increase as stars ascend the red-giant branch. The assumption that the emission is formed in a fully ionized gas by recombination is purely arbitrary, and uncertainties in the assumed stellar radii represent another source of error, which has already led to a disagreement of an order of magnitude (Cohen, 1976; Mallia and Pagel, 1978). The observation of asymmetric blue-shifted line cores (Peterson, 1981, 1982) implies that the outer envelopes of some red giants in globular clusters are expanding, but not necessarily that matter is escaping.

Infrared Dust Emission

Emission by silicates in a broad band centered at $9.7 \mu\text{m}$ is a common occurrence in the spectra of late-type O-rich giants and supergiants. In the carbon stars, a similar but narrower band near $11 \mu\text{m}$ is probably radiated by SiC, while a third species of unknown composition contributes to the continua of some, but not all, C and S stars. The silicate feature is the most useful indicator of mass loss in the middle infrared. In the far infrared, thermal continuum emission near $400 \mu\text{m}$ by silicate and carbon grains is the most promising determinant of dust mass loss from highly evolved stars. We consider first the silicate emission at $10 \mu\text{m}$ and next the continuous emission at sub-millimeter wavelengths.

Emission by Silicates at 10 Microns. Figure 5-5 shows the excess emission observed in the $10\text{-}\mu\text{m}$ region of red-giant spectra, as compared with blackbody emission at the stellar

temperature. Basically, one tries to extract the optical depth of the dust grains at $10\ \mu\text{m}$ from the amplitude of the excess emission, bearing in mind that the amount radiated also depends on the temperature of the dust. The dust temperature is determined by the composition of the grains and their absorbing properties at the shorter infrared wavelengths where most of the stellar radiation is concentrated. The radial optical depth $\tau(10\ \mu\text{m})$ is then used to calculate the column density of dust,

$$\tau(10\ \mu\text{m}) = a^2 \cdot Q(10\ \mu\text{m}) \cdot N_c, \quad (5-8)$$

where a is the radius of a grain, Q is the absorption efficiency at $10\ \mu\text{m}$, and N_c is the column density of silicate grains per cm^2 . If

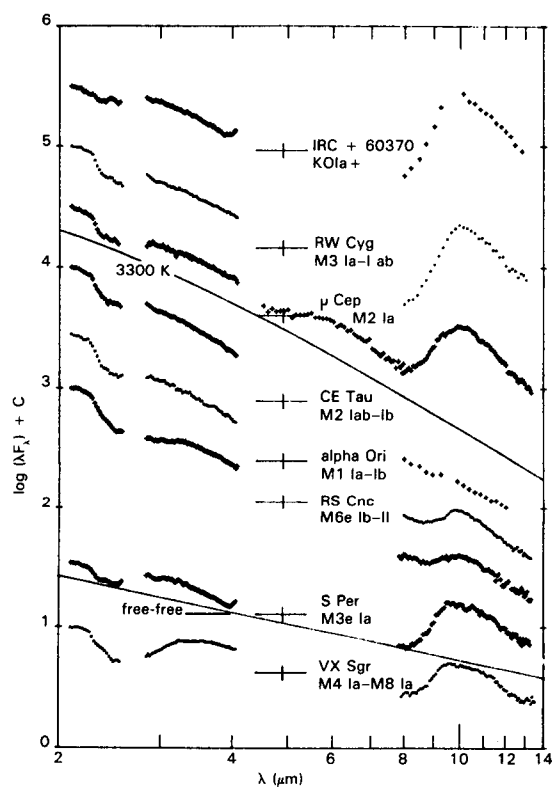


Figure 5-5. Spectral energy curves for K and M supergiants in the 2- to 3- μm region. The excess emission near $10\ \mu\text{m}$ is clearly seen. For comparison, curves for a 3300 K blackbody and for free-free emission are drawn on a relative scale (Merrill, 1977).

values of a and Q are known or assumed, N_c may be found from Equation (5-8). Next, the column density of hydrogen may be inferred from: (a) the assumed grain composition, (b) a judgment as to the fraction of a given element that may have condensed on the grains, and (c) an estimate of the abundance of that element relative to hydrogen. Finally, the mass-loss rate is calculated from Equation (5-3) with the aid of expansion velocities derived from optical spectra and estimates of the inner shell radius by one means or another.

The most uncertain step in the analysis is the derivation of $\tau(10\ \mu\text{m})$ from the observed IR emission, which requires knowledge of half a dozen other parameters, and is therefore strongly model-dependent (Hagen, 1978):

1. The dust temperature distribution is determined by the equilibrium between the absorption of stellar radiation at wavelengths smaller than $5\ \mu\text{m}$ and the emission at longer wavelengths. Knowledge of grain compositions and absorption efficiencies are of critical importance. In discussions of grain temperatures, a distinction is usually made between so-called "clean" silicates, which are relatively pure and have highly developed crystalline structures, and "dirty" silicates, which have disordered lattices (e.g., natural hydrous silicates in carbonaceous chondrites) or are coated with impurities such as graphite. Clean silicates are transparent to short infrared wavelengths, whereas the dirty silicates are strong absorbers at these wavelengths. Jones and Merrill (1976) showed that pure silicate grains reach an equilibrium temperature that is too low to reproduce the observed $10\text{-}\mu\text{m}$ feature. The introduction of impurity (dirty silicates) raises the short-wave efficiency and warms the grains.
2. The absorption efficiencies are well known for relatively few minerals, and

although they are reasonably independent of composition at $10\ \mu\text{m}$, they differ from one mineral to another by several orders of magnitude at wavelengths less than $5\ \mu\text{m}$, where the stars radiate most of their energy. The temperature distributions are correspondingly uncertain.

3. For given optical depth, the size of the shell, particularly the inner radius, determines the flux at $10\ \mu\text{m}$.
4. The density distribution for dust grains is another important input. It is usually assumed that the density falls off as r^{-a} , where $a = 2$ for constant velocity. Hagen (1978) prefers $a = 1.5$, but nevertheless assumes constant velocity.
5. The small-grain approximation (Shaw, 1975) is usually chosen to fix the grain size, with $a = 0.05$ to $0.1\ \mu\text{m}$. In this range, $a \ll \lambda$, and $Q(\text{abs}) \propto a$. The dust temperature is independent of grain size, since both the energy absorbed per unit mass and the energy emitted are proportional to the grain volume.
6. Hagen (1978) took partial account of radiative-transfer effects by including a correction for self-absorption of starlight by the dust, but a more exact treatment is required when $\tau(10\ \mu\text{m})$ is greater than unity (Rowan-Robinson and Harris, 1983a).

The extensive survey of IR circumstellar emission by Gehrz and Woolf (1971) was based on IR photometry at 3.5 , 8.4 , and $11\ \mu\text{m}$. The color $3.5\ \mu\text{m} - 8.4\ \mu\text{m}$ was taken as a measure of silicate emission and the color $8.4\ \mu\text{m} - 11\ \mu\text{m}$ as a measure of optical depth. Gehrz and Woolf avoided many of the problems of the data analysis by adopting a model of a thin spherical shell with temperature T at a distance R from the center of the star. When the color $8.4\ \mu\text{m} - 11\ \mu\text{m}$ is plotted against the color 3.5

$\mu\text{m} - 8.4\ \mu\text{m}$, comparison with model curves gives both $\tau(11\ \mu\text{m})$ and $(R/R_*) (T/T_*)^{-1/2}$. Optical depths for class Ia supergiants were found to be 0.1 to 0.2, as compared with about unity for Miras and about 0.25 for SRb variables. The adoption of a dust temperature of 900 K for all calculations led to estimates for the inner radii of shells of about $4 R_*$ for typical red giants and Miras and about $20 R_*$ for supergiants.

In a study of mass loss from nine stars, which included giants, Miras, and supergiants, Hagen (1978) computed optically thin model dust shells (Dyck and Simon, 1975) to calculate infrared fluxes, making some allowance for self-absorption. After calculating a number of emission profiles as a function of τ for assumed values of the other model parameters, Hagen chooses a value of τ by comparing the predicted and observed emission bump heights and evaluates the dust column density from Equation (5-8). The hydrogen column density then follows from the assumed grain composition. In calculating mass-loss rates from total column densities, Hagen (1978) took as inner shell radii the distances at which silicate grains condense, which vary from $1.2 R_*$ for a 2500 K star to $1.9 R_*$ for a 3600 K star. As Hagen points out, these small distances are inconsistent with the analysis of the optical line profiles, which were modeled on the assumption that the radius of the inner shell is larger than R_* by at least a factor of 3. In a more recent survey of 42 red giants and supergiants (Hagen et al., 1983), the inner shell radius is set at a uniform value of $10 R_*$ for all stars.

In the same paper, Hagen (1978) also derives hydrogen column densities from optical lines, using Sr II for the cooler stars later than M5 and Sr II, Ba II, and Sc II for the early M stars. Since she assumes that the same fraction of all elements is condensed into grains, the addition of the two values of $N(\text{H})$ gives the total column density of CS matter, and the ratio of the two is the relative proportion of metals existing as gas and dust, respectively. It is hard to understand how two elements such as Sr and Si, with fractional abundances differing by five

orders of magnitude, can be condensed on grains in the same proportions. At the very least, the investigation should be repeated, using optical observations of elements with abundances comparable to that of Si.

One of the principal conclusions from these studies is that the total quantity of CS gas derived from the Sr II 4077 Å line is uncorrelated with the quantity of CS dust implied by the strength of the 10- μ m silicate feature. Such a correlation is expected from the theory of dust-driven mass loss (see Deguchi, 1980), but its absence may not be too significant in view of the many uncertainties in the derivation of dust column densities. Moreover, the use of a single line, 4077 Å of Sr II, as a measure of total gas content implies far more confidence in ionization theory and in solar-like abundances than is warranted. It appears that the fraction of metals in the form of dust and gas, respectively, are not at all well determined.

Submillimeter Dust Emission. In principle, the rate of mass loss in the form of dust may be estimated more directly from the thermal emission of the dust at submillimeter wavelengths than from the 10- μ m silicate feature. Sopka et al. (1984) have reported observations of 17 evolved stars, obtained with the United Kingdom (U.K.) infrared telescope on Mauna Kea at an effective wavelength of 400 μ m. At this wavelength, the dust is optically thin, and moreover, the dust emission follows the Rayleigh-Jeans law. Consequently, uncertainties in grain temperature are not as serious as at shorter wavelengths. Nine of the objects were detected, and rates of mass loss, varying in amount from about 10^{-7} to $7.6 \times 10^{-6} M_{\odot}$ /yr, were estimated from the fluxes and are listed in Table 5-2. The greatest potential sources of error are the distance and $\kappa(400 \mu\text{m})$, the cross section per unit mass of the grains. Although the composition of both carbon and silicate grains is unknown, several lines of evidence (Draine, 1981; Rowan-Robinson and Harris, 1983b; Jura, 1983a) suggest that carbon in the interstellar medium is amorphous rather than crystalline in structure and that the

silicates are likely to be amorphous as well. The slopes of the far-IR to submillimeter spectra of both carbon-rich and oxygen-rich stars also support the conclusion that both carbon and silicate grains have amorphous structures. Thus, Sopka et al. (1984) adopt a common value of $\kappa = 20 \text{ cm}^2$ for both carbon-rich and oxygen-rich stars, which is estimated to be accurate to within a factor of 3, and is about an order of magnitude less for crystalline materials. The seventh column of Table 5-2 gives the ratio of mass lost in the form of gas and dust, respectively, which is seen to be consistent with the interstellar value of 100.

It is noteworthy that the largest values of \dot{M}_d are found for the bipolar objects, OH 231.8 + 4.2, CRL 2688, CRL 618, the planetary nebula NGC 7027, and VY CMa, in all of which the flows are highly anisotropic. It might be believed that analysis of such objects based on spherical symmetry might give incorrect results, but Jura's (1983b) calculation of mass loss from oblate ellipsoids shows that the rates are not greatly different from values derived by assuming spherical symmetry.

Millimeter Waves

Since it was first detected a few years ago (Zuckerman et al., 1977, 1978; Lo and Bechis, 1977; Morris et al., 1979; Morris, 1980; see also Rieu, this volume, for an up-to-date review), thermal millimeter-wave radiation in rotational lines of molecules has become an increasingly important tool for studying mass loss from red giants. The CO lines have been most widely used in rate determinations. The 1-0 line has been detected in 50 stars, mostly of types M, S, and C (Knapp and Morris, 1984), and the 2-1 line in 17 of the same objects (Knapp et al., 1982). Such lines are particularly valuable for rate determinations because they are formed far from the star, where the flow is likely to have attained both its terminal velocity and spherical symmetry. One disadvantage is that they appear in emission, and hence the mass of CO in the envelope must be derived from detailed models in which the square of the distance is a free

Table 5-2
Mass-Loss Rates and Expansion Velocities of Selected Red-Giant Stars

Star	Spectral Class	\dot{M}_g	V_{exp} (km/s)	\dot{M}_d	\dot{M}_g/\dot{M}_d	Ref. †
ϰ Per	M4 II-III	0.012	7			2
119 Tau	M2 Ib	0.24	7			2
α Ori	M2 lab	4	10			3,4,5
6 Gem	M1-M2 Ia-lab	2.1	8			2
α Sco	M1.5 lab	5.4	9			2,6
α Her	M5 Ib-II	0.11	8			2,7
δ ² Lyr	M4 II	0.048	7			2
R Lyr	M4-5 III	0.014	5			2
μ Cep	M2 Ia	1.0	9			2,4
δ Sge	M2 II	0.02	28			8
IRC + 10011	M8	14	24	0.07	200	9,10
ο Cet	M6e	0.65	4			9
NML Tau	M	5.1	28			9
S CMi	M7e	6.3	18			1
RS Cnc	M6 Ib-II	0.29	11			9
R LMi	M7e	1.0	6			1
R Leo	M8e	0.092	7			9
RX Boo	M7e	0.38	8			9
NML Cyg	M6 III	1.8	21	0.058	31	1,10
R Cas	M7e	0.66	11			1
R And	S6e	0.37	15			9
W Aql	S	9.8	20			9
χ Cyg	S7e	0.18	8			1
IC 418	PN	5.0	17			1
NGC 6543	PN	5.1	14			1
NGC 7027	PN	110	22	1.3	85	9,10
R Scl	C	31	16			9
IRC + 50096	C	6.3	18			9
CRL 618	C	77	18	0.85	90	9,10
CRL 865	C	23	14			9
IRC + 10216	C9	55	17	0.17	320	9,10
CIT 6	C4	3.0	17			9
IRC - 10236	C	47	10			9
V Hya	C6 ₃ e	4.6	18			9
IRC + 20326	C	23	10			9
CRL 2155	C	17	20			9
CRL 2199	C	13	15			9
IRC + 20370	C7	10	9			9
V Cyg	C7e	25	14			1
CRL 2688	C	160	19	2.3	70	9,10
IRC + 40485	C	17	13			1
CRL 3068	C	7.3	14	0.086	85	9
IRC + 40540	C8	24	15			9
OH231.8 + 4.2		130	68	7.6	17	9,10

* \dot{M}_g and \dot{M}_d are rates derived for gas and dust, respectively, in units of $10^{-6} M_{\odot}/\text{yr}$.

† References: 1. Knapp et al. (1982); 2. Sanner (1976); 3. Bernat et al. (1979); 4. Hagen et al. (1983); 5. Maunon et al. (1984); 6. Hjellming and Newell (1983); 7. Reimers (1977); 8. Reimers and Schröder (1983); 9. Knapp and Morris (1984); 10. Sopka et al. (1984).

parameter; another is the uncertainty in the composition ratio CO/H_2 , which may, in some cases, be derived indirectly from observation (see below). Circumstellar chemistry is a new field of research, which is not yet on a firm quantitative basis. (See the review by Glassgold and Huggins in this volume.)

Figure 5-6 shows typical spectra in the region of the $\text{CO } J = 2-1$ line for Betelgeuse and IRC + 10011. As shown by Morris (1975), the profiles of emission lines from unresolved spherical gas clouds expanding at constant velocity are flat-topped, as in Betelgeuse, when the cloud is optically thin, and parabolic, as in IRC + 10011, when the cloud is optically thick. The width of the profile at zero intensity or power is twice the expansion velocity, V_{exp} , whereas the velocity at the center of the line is the systemic, or center-of-mass velocity of the star, V_c . For Betelgeuse, the derived velocities are $V_{exp} = 15.3 \pm 2.5$ km/s and $V_c = 18.8 \pm 2.5$ km/s (Knapp et al., 1980), in good agreement with the optical values $V_{exp} = 16.5$ and 10.0 km/s (Goldberg et al., 1975; Bernat et al., 1979) and $V_c = 21$ km/s (Adams, 1956). The expansion velocity derived from the emission profile apparently corresponds to the larger of the two displacements observed in optical absorption spectra of α Ori. The absence of emission from the inner shell can be understood (Knapp et al., 1980) if the shell is much closer to the star than proposed by Bernat et al. (1979), $8 R_*$ rather than $150 R_*$. Moreover, spatial mapping of the millimeter-wave emission from Betelgeuse gives a radius of about $400 R_*$ for the outer shell, again much smaller than the value of about $2000 R_*$ found by Bernat et al. (1979). Goldreich (1980) has pointed out that the gas in the circumstellar shell is heated by the drag force between gas and dust and not by the thermal dust temperature. It is therefore incorrect to equate the excitation temperature with the equilibrium temperature of the dust, at least for those objects in which the rate of mass loss and therefore the density are relatively low (Morris, 1980).

Theoretical models of circumstellar envelopes around red giants, in which rates of mass

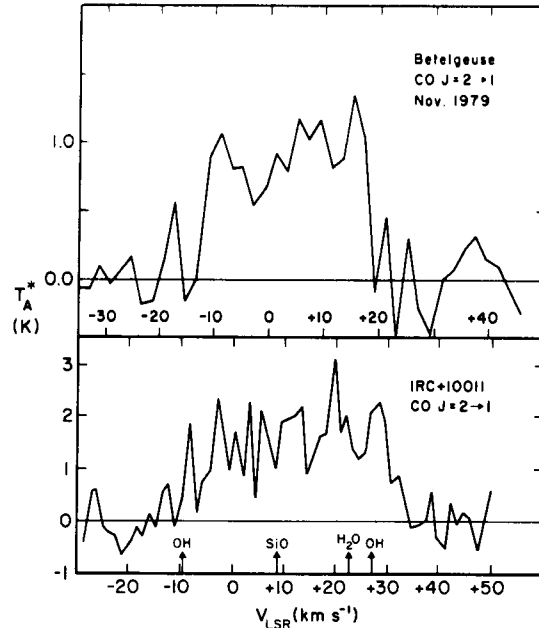


Figure 5-6. Spectra in the region of the $\text{CO } J = 2-1$ line at 230 GHz for α Ori (top) and IRC + 10011. Possible blends with lines of other molecules are indicated (Knapp et al., 1982).

loss and chemical compositions are parameters to be derived from molecular line observations, have been calculated by Goldreich and Scoville (1976) for OH/IR stars, by Kwan and Hill (1977) and Kwan and Linke (1982) for the carbon star, IRC + 10216, and by Morris (1980; see also Morris and Alcock, 1977) for a wide range of stellar parameters. In all of these models, mass loss is assumed to be driven by radiation pressure on dust grains in a spherically symmetric atmosphere. The gas temperature distribution is determined by the balance between heating by collisions with grains and cooling by adiabatic expansion and by the emission of H_2O in O-rich stars and of CO in carbon stars. Because most of the CO emission occurs hundreds of stellar radii from the star, Kwan and Linke (1982) assume constant outflow velocity and use the Sobolev approximation to solve the radiative-transfer problem. The solution contains three free parameters: \dot{M} ,

the rate of mass loss, \dot{Q} , the momentum transfer efficiency factor averaged over the continuum energy distribution, and $(\text{CO})/(\text{H}_2)$, the abundance ratio carbon monoxide to molecular hydrogen. It is expected that, in the circumstellar envelopes of the cooler late-type stars, hydrogen will be predominantly in molecular form (Knapp and Bowers, 1983). The dust grains are assumed to constitute 1 percent of the mass and to have a density of 1 gm/cc. Since these quantities always enter with \dot{Q} , their uncertainties are lumped together with the uncertainty in \dot{Q} , which may be checked by calculating the optical depth of the dust and comparing it with that of infrared observations.

Morris (1980; see also Morris and Alcock, 1977) bases his model on temperature and velocity distributions derived from their dust model by Goldreich and Scoville (1976). For example, the velocity law is:

$$V \approx V_{\text{Term}} - 0.37 \times 10^{16}/r, \quad (5-9)$$

for $r > 10^{15}$ cm, equivalent to $20 R_*$ for Betelgeuse.

Morris solves the coupled equations of radiative transfer and statistical equilibrium to calculate the radial distribution of the populations in the lowest 11 rotational levels of both the first and second vibrational levels of CO. The processes contributing to the level excitations are:

1. The millimeter-wave radiation field, in part from the 3 K background and in part from diffused CO line radiation.
2. The 4.6- μm radiation field exciting the $v = 0-1$ transitions. The central star is assumed to be a blackbody with a temperature of 2000 K and a radius of 5×10^{13} cm, and a parameter, W , is supposed to measure the amplification of the 4.6- μm radiation by the surrounding dust. No account appears to have been taken of the weakening of the stellar radiation field by CO absorption in the photosphere.
3. The levels are also excited by collisions with H_2 molecules, the results being insensitive to the assumed temperature distribution.

Results are presented for the central intensities of the transitions $J = 1-0$, $2-1$, and $3-2$ as a function of \dot{M} (the mass-loss rate), W (the measure of 4.6- μm luminosity), and f (the fractional abundance of CO relative to H_2), and for the beamwidths of the 11-m National Radio Astronomy Observatory telescope and the 10-m Owens Valley Radio Observatory telescope. For a completely unresolved envelope, the brightness temperature is inversely proportional to the distance squared. Actually, both of the above telescopes can resolve envelopes at distances closer than 1000 parsecs, which means that an increase in distance is partially compensated by an increase in the surface area intercepted by the beam. Therefore, the peak surface brightness falls off less rapidly than as D^{-2} .

The results show that, when the product $f \times \dot{M} < 10^{-9}$, the envelope is optically thin both in the rotational lines and in the 4.6- μm lines. The line profiles are flat for $D > 1$ kpc and become double-peaked as D decreases because the outer parts of the emitting region are no longer within the telescope beam. When $f \times \dot{M} > 2 \times 10^{-9}$, the envelope is optically thick in both rotational and vibrational lines. Increased density causes the excitation to be dominated by collisions with H_2 . Finally, when $f \times \dot{M} \sim 10^{-9}$, weak maser emission may occur.

It might be believed that only the product $f \times \dot{M}$ could be derived from comparing model calculations with observations, but that is usually true only in cases in which the levels are excited purely by radiation. Otherwise, the same value of the product $f \times \dot{M}$ may produce profiles of quite different intensity and shape (double-peaked, flat, or parabolic) depending on the relative values of f and \dot{M} . The reason is that the value of \dot{M} is a measure of the density, which controls the rate of collisions and

thus the excitation temperature. An increase in excitation temperature increases the size of the observed emitting region and therefore modifies the shape of the profile. Thus, detailed modeling of emission-line profiles can yield both the mass-loss rate and information on the chemical composition.

Another type of modeling, which seeks to combine optical and radio observations, was conceived by Jura and Morris (1981) and applied to the shell of Betelgeuse. The model is derived from observations of the 2-1 line of CO (Knapp et al., 1980) combined with measures of the surface brightness of the shell in the monochromatic radiation 7699 Å of K I at distances of 20 to 60 arc-sec from the star (Honeycutt et al., 1980). At such great distances from the star, the ionization of K is controlled entirely by the interstellar radiation field, although modified by dust extinction, or shielding, in the shell itself, and therefore the uncertainty about the stellar radiation field is avoided. The analysis has recently been repeated by Mauron et al. (1984) using new surface brightness measurements made with a Fabry-Pérot etalon and a charge-coupled device (CCD) camera. The method yields the radial density distribution of potassium and of hydrogen if the solar abundance ratio is assumed. A by-product of the analysis is the abundance ratio carbon/potassium. So far, such optical surface brightness distributions have been measured only for the star Betelgeuse.

In their survey of mass loss from 17 evolved stars, Knapp et al. (1982) avoided detailed modeling by putting the stars into two categories, those with optically thick and optically thin envelopes, respectively, and deriving simple expressions for the mass-loss rate in terms of antenna temperature, T_A^* , expansion velocity, V , and distance, D . The expressions are designed to fit the IRC + 10216 model of Kwan and Hill (1977) and Kwan and Linke (1982) as a prototype for the optically thick envelopes and the α Ori models of Bernat et al. (1979) and Jura and Morris (1981) as typical for optically thin envelopes. The models predict that the ratio of antenna temperatures of the 2-1 and

1-0 lines of CO should be about 3 in optically thick envelopes and several times larger for optically thin shells. According to this criterion, 15 of the 17 shells were shown to be optically thick, the only exceptions being Betelgeuse and Mira.

In their optically thick approximation, Knapp et al. (1982) assume that each source is a sphere of constant surface brightness, the radius being fixed by the gas density at which the CO lines are no longer thermalized. However, Jura (1983b) has shown that the outer optically thin regions of the sources cannot be neglected, since they contribute substantially to the total flux. Allowance for this effect reduces Knapp et al.'s mass-loss rates by a factor of 2 to 3. A further reduction of about 30 percent becomes necessary when the effects of dust shielding and molecular self-shielding are considered (Jura, 1983b). Jura's analysis leads to a less steep dependence of mass loss on distance, $D^{3/2}$, rather than D^2 as found by Knapp et al. (1982).

A new survey by Knapp and Morris (1984) has detected 50 sources in the 1-0 line. The analysis has been carried out with a minimum of simplifying approximations, and the results are probably more reliable than those of Knapp et al. (1982). As before, general expressions for T_A^* were derived for both optically thin and optically thick cases, respectively. For both cases, the antenna temperature is a function of \dot{M} , D , f , and r_m , the maximum extent of CO in the envelope. In optically thin objects, T_A^* also depends on the IR flux, W . For most objects, the model profiles are in satisfactory agreement with observations, but a few optically thin shells, including those of α Ceti and α Ori, presented problems that require further study. In view of the many free parameters in the theory, the results must still be regarded with some caution.

Microwave Emission

VLA measurements of radio emission at centimeter wavelengths from the supergiants Betelgeuse (Newell and Hjellming, 1982) and

Antares (Hjellming and Newell, 1983) are consistent with emission of an optically thick thermal radio spectrum emitted by an extended slightly ionized chromosphere extending to several stellar radii. In addition, the observations suggest that the wind from Antares is ionized by the Lyman continuum radiation of the companion B2.5 V star. Figures 5-7a and 5-7b are 4.885-GHz images of the Sco system made with the VLA, showing the unresolved M star on the left and the nebulosity surrounding the B star, the location of which is marked by a cross. Figure 5-7c is a theoretical model of the ionized portion of the Antares stellar wind, which is created by the ultraviolet flux from the B star. The agreement between theory and observation is most convincing and suggests a new method for measuring the rate of mass loss from an M supergiant. Hjellming and Newell (1983) point out that, at the ionization front between the neutral and ionized hydrogen, the number of neutral hydrogen atoms flowing per square centimeter across the ionization front must equal the attenuated Lyman continuum photon flux which ionizes the gas. Thus,

$$N_1 v_1 = L(\text{ly}) \cdot \exp(-\tau_1) / 4\pi \cdot r_1^2 \quad , \quad (5-10)$$

where N_1 and v_1 are the hydrogen density and velocity of the wind at distances of R_1 and r_1 from the M and B stars, respectively; τ_1 is the optical depth for the Lyman radiation between the ionization front and the star, assumed to be unity; and $L(\text{ly})$ is derived from a model of the microwave radio emission from the star. Its value is proportional to the square of the stellar distance and to the $-1/6$ power of the electron temperature. Since the mass-loss rate is:

$$\dot{M} = 4\pi \cdot \rho_1 \cdot v_1 \cdot R_1^2 \quad , \quad (5-11)$$

where ρ is the density, the expansion velocity may be eliminated, and \dot{M} is given by:

$$\dot{M} = (\rho_1/N_1) \cdot L(\text{ly}) \cdot \exp(-\tau_1) \cdot (R_1/r_1)^2 \quad . \quad (5-12)$$

Thus, the mass-loss rate may be derived entirely from observed quantities and straightforward application of the theory of H II regions.

Because systems like α Sco are uncommon, Hjellming and Newell's (1983) method will not have wide application. Moreover, only the hottest late-type giants will have winds in which most of the hydrogen is ionized. Thus, the microwave flux from M giants and supergiants will not be useful for the determination of mass-loss rates unless there is an independent means for measuring the fraction of ionized hydrogen. α Ori is known to emit weak microwave radiation (Newell and Hjellming, 1982) from an extended warm chromosphere in which the flow is probably accelerating, but in which the fractional ionization cannot be more than 0.01 to 0.10. The same fraction has been found for α^1 Her (Drake and Linsky, 1984). Spergel et al. (1983) observed 31 evolved red giants with known high rates of mass loss with the VLA at 5 GHz and detected emission from only four stars. Upper limits of about 10^{-3} were derived for the fractional hydrogen ionization. On the other hand, the probable detection of α Boo, also with the VLA at 6 cm (Drake and Linsky, 1984), implies a mass-loss rate of $1 \times 10^{-10} M_\odot/\text{yr}$, which indicates that hydrogen in the wind is well ionized.

OH/IR Masers

The subject of red-giant masers has recently been reviewed by Elitzur (1981). Maser radiation at radio frequencies, which is usually found in oxygen-rich giants and supergiants of spectral types later than M5, is emitted by SiO, H₂O, and OH molecules. The SiO radiation is emitted by excited vibrational levels, which are pumped by collisions, and therefore must be located in the lower atmosphere of a star. The OH lines, at 1612, 1665, 1667, and 1720 MHz, originate from the ground vibrational state and

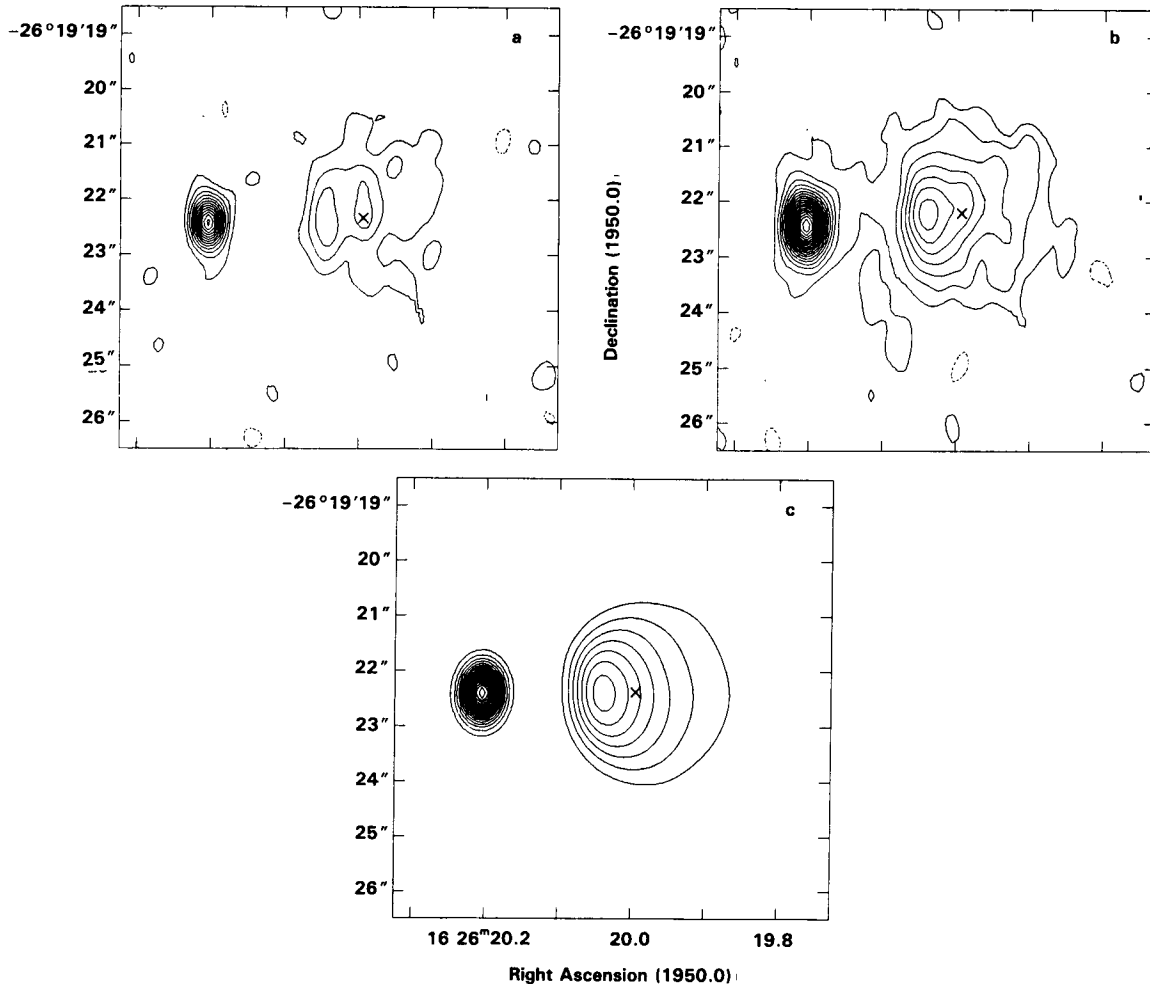


Figure 5-7. Images of the α Sco radio source made with the VLA at 4.885 GHz. The unresolved M star is at the left, and the position of the B star is marked by a cross at the right. (a) and (b) are images constructed with different methods of weighting, and (c) is a theoretical model of an H II region produced in the wind of the M star by UV photons from the B star (Hjellming and Newell, 1983).

are pumped by IR radiation, as evidenced by the variations in phase of IR and OH emission (Harvey et al., 1974). Three of these four lines have been found to emit maser radiation in late-type stars, the so-called main lines at 1665 and 1667 MHz, and the satellite line at 1612 MHz. Those stars with stronger main lines are classified as Type I and those with stronger satellite lines as Type II. We shall be concerned here only with Type II masers because model calculations show that the satellite line is emitted only by stars with very high rates of mass loss. The enormous extent of maser shells has been

verified independently by different methods. Thus, Baud (1981) observed, with the VLA, extended OH emission from the source OH 26.5 + 0.6 over a diameter of 4.6×10^{16} cm. Jewell et al. (1980), making use of the phase relation between variations in the OH 1612-MHz emission originating from the front and back of the shell, derived a diameter of $(6.6 \pm 1.4) \times 10^{16}$ cm for the maser shell around IRC + 10011.

Some typical spectra in the region of the 1612-MHz line are shown in Figure 5-8. The

two peaks originate from the approaching and receding halves of the shell, respectively. Hence, the separation of the peaks measures twice the expansion velocity, and the velocity half way between the peaks is the systemic velocity of the star. Mass-loss rates are determined from these observations on the assumption that the mechanism is radiation pressure on dust grains, which is highly likely for stars with such thick dust shells. If radiation pressure on grains is much larger than all other forces, such as gravitation, it can be shown that the equation of motion, when combined with the equation of continuity and the definition of optical depth (Elitzur, 1981), reduces to:

$$\dot{M} = L \cdot \tau_D / Vc \quad , \quad (5-13)$$

where L is the mean IR flux, V is the terminal expansion velocity, c is the velocity of light, and τ_D is the effective optical depth of the dust through the shell in response to radiation pressure. Its value is on the order of 2 for dense shells.

A second expression for the mass-loss rate may be obtained by integrating the equation of motion to obtain an expression for the terminal velocity, which, when inserted into the equation of continuity, gives (Salpeter, 1974):

$$\dot{M} = 2\pi \cdot R_o \cdot V \cdot \tau_D / \kappa_D \cdot f \quad , \quad (5-14)$$

where τ_D is the optical depth at a given wavelength, say, $9.7 \mu\text{m}$, κ is the mass absorption coefficient at the same wavelength, f is the fraction of the total mass in the form of dust, and R_o is the radius at which dust forms. Forrest et al. (1978) have used both equations to obtain estimates of mass loss from OH26.5 + 0.6. From Equation (5-14), with $\tau > 6$, $\kappa(9.7 \mu\text{m}) = 3000$, $R_o/r_* > 3$, and $r_* = 6.5 \times 10^{13}$ cm, $\dot{M} > 1.5 \times 10^{-5} M_\odot/\text{yr}$. Similarly, Equation (5-13), with $L = 10^4$, which is appropriate for Miras, $V = 13$ km/s, and $\tau = 3$, gives \dot{M}

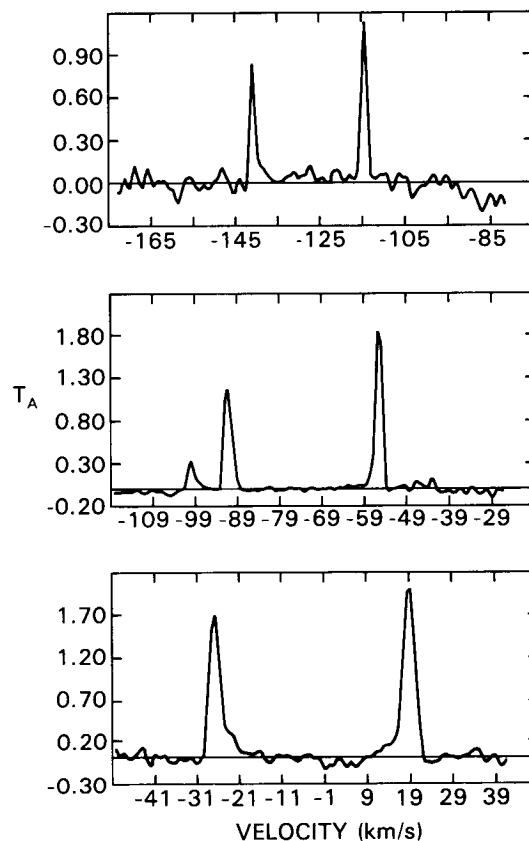


Figure 5-8. Spectra of Type II OH sources at 1612 MHz: Top: OH 1.5-0.0; middle: OH 2.2-1.7; bottom: OH 2.6-0.5. The left and right peaks arise from the approaching and receding halves of the shell, respectively (Baud et al., 1979).

$> 4.5 \times 10^{-5} M_\odot/\text{yr}$. Mass-loss rates calculated for OH/IR stars with Equation (5-13) appear in Table 5-3.

Results

Compilations of mass-loss rates for late-type stars, derived by the methods described above, will be found in Gehrz and Woolf (1971), Reimers (1975a, 1975b), Sanner (1976), Bernat (1977), Hagen (1978), Werner et al. (1980), Knapp et al. (1982), Hagen et al. (1983), Jura (1983b), Baud and Habing (1983), Engels et al. (1983), Sopka et al. (1984), Pottasch (1984),

Table 5-3
Periods, Expansion Velocities, and Mass-Loss Rates of OH/IR Stars
Calculated from Equation (5-13)

Star	Period (days)	V_{exp} (km s ⁻¹)	\dot{M} (10 ⁻⁶ M _⊙ /yr)	Ref. *
R Aql	280	6.5	0.8	1
U Ori	372	4	0.3	1
RR Aql	394	6.5	0.5	1
WX Ser	425	7.5	1	1
OH31.7 - 0.8	510	13	10.9	2
OH26.4 - 1.9	540	12	5.2	2
OH19.2 - 1.0	610	15	24	2
OH28.7 - 0.6	640	18	22.4	2
OH45.5 + 0.1	720	18	4	2,3
OH39.9 + 0.0	770	15	28.7	2
OH30.1 - 0.2	970	18	23	2,3
OH30.7 + 0.4	1140	18	8.1	2
OH26.2 - 0.6	1330	22	33.2	2
OH26.5 + 0.6	1630	14	75	2,3
OH32.8 - 0.3	1750	16	60	2,3

*References: 1. Pottasch (1984); 2. Engels et al. (1983); 3. Werner et al. (1980).

and Knapp and Morris (1984), among others. A useful tabulation of circumstellar line strengths and velocity displacements for 61 red giants is found in Boesgaard and Hagen (1979). Even for such well-studied stars as α Ori, α Sco, and IRC + 10216, published values of the mass-loss rates differ by factors of 10 to 100, and hence, it does not seem useful to present them all in tabular form. In many cases, however, discordant values can be weeded out for known reasons, and the remaining values, although still uncertain by factors of perhaps 2 to 10, serve a useful purpose in setting constraints on mechanisms and evolutionary processes.

Thus, Tables 5-2 and 5-3 are compilations of mass-loss rates of evolved stars selected,

because they seemed to be relatively well determined, from among several different classes of stars. Table 5-2 contains expansion velocities and mass-loss rates for early- and late-type M stars, for carbon stars, and for a few S stars and planetary nebulae. Rates for the early M stars have been derived mainly from optical data, and the selection of the best values can be a matter of personal taste. α Ori is a case in point. Jura and Morris (1981) and Maun et al. (1984) used exactly the same method of analysis, combining data on CO line emission with surface brightness measurements in neutral potassium, but their rates differ by a factor of 4 because the surface brightness distribution of K I emission measured by Maun et al. (1984) differed considerably from that of Honeycutt

et al. (1980). It should be noted that the abundance ratio K/C found by Jura and Morris (1981) was 25 times larger than the solar value, but Maunon et al. (1984) reduced this discrepancy by a factor of 6. A reduction in the C/H ratio by a factor of 1 to 5 would not be unexpected for processed material. For the later spectral types and the carbon stars, the most reliable rates are probably those from rotational lines of CO. When available, the most recent values of Knapp and Morris (1984) have been adopted. The data show several clear trends:

1. Among the early M stars, rates for the supergiants exceed those for the giants by a factor of 10 or more.
2. Rates for the Miras and planetary nebulae are comparable to those for the early-type supergiants, but the value for NGC 7027 is at the extreme upper end of the range.
3. Knapp et al. (1982) found that the rates for the carbon stars were 25 times larger, on the average, than those for the O-rich stars, but this result is not borne out by the newer analysis of Knapp and Morris (1984), who allowed for the presumably higher CO abundance in C-rich stars and included the effects of excitation by stellar IR on the optically thin objects. Thus, if $f = 3 \times 10^{-4}$ for oxygen Miras and 8×10^{-4} for the carbon stars, the range of rates of mass loss found for the two groups of stars is about the same. The results of the Knapp and Morris (1984) survey are summarized in their Figure 16 in the form of histograms in which the number of stars per pc^3 is plotted against \dot{M} .
4. The M and S stars show considerable scatter in their expansion velocities, with values from 4 to 28 km/s, whereas among the carbon stars, v_{exp} is essentially confined between 10 and 20 km/s.

Table 5-3 is a compilation of periods, expansion velocities, and mass-loss rates of OH/IR stars, the rates having been calculated from Equation (5-13). The table contains four OH/IR objects optically identified as Miras, together with 11 unidentified OH/IR stars. The results for the OH/IR stars can be better understood in view of recent studies of these fascinating objects. About 350 OH masers are known (Engels, et al., 1981), of which less than one-third have been identified optically, most as M-type Miras but also M supergiants, semi-regular variables, and some very red IRC sources. A recent survey of about 200 OH/IR stars (Engels et al., 1981) revealed that all OH/IR stars are variable, with amplitudes up to two magnitudes in the K band. At least one-half the stars have longer periods than those of Miras or IRC sources, with values up to 1600 days or more. It now seems to be well established (Baud and Habing, 1983; Engels et al., 1983) that the optically identified OH/IR stars and the unidentified sources form a continuous sequence of Mira variables extending from the optical objects with periods up to about 400 days to the unidentified sources with periods up to nearly 2000 days. As seen in Table 5-3, the expansion velocities along this sequence increase on the average from <10 km/s for optical Miras to 22 km/s. From statistical studies of velocity dispersions and galactic concentrations, Baud et al. (1981) found the expansion velocities to be correlated with age and main-sequence mass in the sense that small velocities go with small mass.

Thus, the progression with period is also one with main-sequence mass from about $0.5 M_{\odot}$ for the optical Miras to $6.5 M_{\odot}$ for the OH/IR sources with the longest periods. The mass-loss rates from unidentified OH/IR stars are also strikingly higher, and the increase occurs rather abruptly at periods over 400 days. There appears to be a threshold period beyond which the rate of mass loss suddenly increases by a factor of 10, and the star becomes enveloped in an opaque dust cloud.

NONSTEADY MASS LOSS

Selected Examples

Evidence is accumulating that, in some stars at least, mass loss may occur sporadically or at a variable rate. The following examples are illustrative rather than complete.

Multiple components of CS lines have been observed in the spectra of a number of red giants and supergiants, chiefly the latter (Sanner, 1976; Bernat, 1981). From a study of CO lines in the 4.6- μm band in nine red giants and supergiants, Bernat (1981) concluded that the multiple components originated in separate mass-loss episodes rather than as intermittent modulations of continuous mass loss, which is favored by Ridgway (1981). The matter is still controversial.

Reimers (1975a, 1975b) noted variability in the K-line profiles of early M giants, stars lying near the transition zone in the HR diagram between stars with low and high rates of mass loss.

Brooke et al. (1974) found evidence for large-scale motions in the atmosphere of α Ori, which appeared to be sporadic in time or position on the stellar surface.

HR 8752 and ρ Cas, two F Ia supergiants with extensive circumstellar shells containing little dust, have undergone dramatic changes in their atomic and molecular spectra in the 2.3- μm region over a period of years (Lambert et al., 1981). During a 5-year period from 1975 to 1979, P Cygni profiles in HR 8752 were transformed into inverse P Cygni profiles, suggesting the fallback of a shell ejected in 1975. The mass-loss rate derived for ρ Cas is very large, exceeding $10^{-3} M_{\odot}/\text{yr}$, leading Lambert et al. (1981) to propose that it is an outburst connected to a peculiar decrease in brightness observed in 1946/1947.

If the stationary atmospheric layer observed by Hinkle et al. (1982) in χ Cyg and other Miras is the source from which mass escapes, the vari-

ations in the thickness of this layer in χ Cygni may be an indication of variable mass loss.

The far-infrared (40 to 250 μm) size of IRC + 10216 (Fazio et al., 1980) suggests more dust at large distances than would be expected for an r^{-2} density distribution. This implies that, about 2000 years ago, the rate of mass loss was twice its present value. Mitchell and Robinson (1980) also derived a relatively shallow density gradient, varying as $r^{-1.3}$. On the other hand, the brightness distribution at 11 μm is consistent with r^{-2} (Sutton et al., 1979). Rowan-Robinson and Harris (1983b) conclude, however, that errors of measurement are too large to rule out the r^{-2} density law.

Optical spectropolarimetry of dust-en-shrouded extreme carbon stars reveals that their circumstellar shells are highly organized (Cohen and Schmidt, 1982). In particular, GL 1403 = IRC + 30219 = CIT 6 seems to show a torus of cool dust and hot bipolar lobes, replenished by outbursts occurring after the minima of the 640-day light variation. Particularly striking were the spectral changes in 1977 through 1980 (Cohen, 1980), when the stellar photosphere nearly disappeared and the spectrum consisted of emission lines of H, He, and forbidden lines. Cohen (1980) suggests that these lines were formed when a recent episode of mass loss collided with the existing circumstellar envelope. These and similar objects may represent the evolution of high-mass carbon variables into bipolar nebulae.

VLA observations of extended OH maser emission for the envelope around OH26.5 + 0.6 show large-scale spatial asymmetries and perhaps a ring-like structure seen edge-on, indicating real density variations in the envelope.

Approximately twelve Type II OH/IR sources have been found to have dust shells of high optical depth and to display deep silicate absorption at 10 μm . Werner et al. (1980) have modeled these shells with an $r^{-1.5}$ density law, whereas Rowan-Robinson (1982) has proposed a double-shell model in which a cool star with a spherically symmetric dust shell expanding at constant velocity is surrounded by a second

shell of cold absorbing dust. The second shell is believed to represent an earlier episode of ejection. The mass of the cold dust is estimated as 4 to 15 M_{\odot} , which implies that the sources are very massive highly evolved stars.

Near-infrared (1.65 to 4.8 μm) speckle interferometry of IRC + 10216 (Dyck et al., 1984) shows the outer regions of the object to be circularly symmetric on scales > 1.6 inch, but at intermediate distances, the brightness distribution is strongly asymmetrical, being more extended north-south than east-west, as found previously by McCarthy et al. (1980). McCarthy et al. also reported variations with time of the apparent envelope size, which have been confirmed by Dyck et al. (1984).

Evidence for Sporadic Mass Loss in α Orionis

α Ori has been relatively well observed for many years, and there is now an impressive amount of evidence for nonsteady ejections of matter at all levels of its highly extended atmosphere and circumstellar shell. At the level of the photosphere, both visible light and radial velocity vary on the average in a period of 5.78 years, apparently arising from pulsation, but these smooth variations are frequently dominated by irregular fluctuations, on a time scale of about 100 days, which often mask the variations associated with the pulsation. (For a summary, see Goldberg (1979, 1984).) Ordered changes in the linear polarization of the visible light have been observed over a number of years (Hayes, 1980, 1981, 1984; Tinbergen et al., 1981). After a lapse of nearly 50 years, systematic monitoring of the photoelectric brightness of the star was resumed in 1979 (Krisciunas, 1982; Guinan, 1983). As shown in Figure 5-9, reproduced from Guinan (1983), the amount of linear polarization and the blue magnitude are at least roughly correlated, which is consistent with asymmetric ejection of matter. Similarly, the absence of a one-to-one correlation between the short-term brightness and velocity variations (Sanford, 1933) makes

it apparent that these changes are not global in nature. The wavelength dependence and time variation of the polarization are qualitatively consistent with the growth of a hotspot, or large convection cell, occupying a few percent of the area of the stellar disk (Schwarz and Clarke, 1984; Clarke and Schwarz, 1984).

The brightness distribution of emission from the inner shell of Betelgeuse within 10 stellar radii also shows pronounced asymmetries (Ricort et al., 1981; Goldberg et al., 1981; Roddier and Roddier, 1983) both in $H\alpha$ light and in the continuum. The asymmetries persist to very large distance scales. Diffraction-limited images of the α Ori dust shell at 10 μm , obtained with the NASA IR telescope on Hawaii (Bloemhof et al., 1984) show a marked asymmetry in the dust distribution, with peak intensity at a distance of 0.9 arc-sec from the star.

The possible association of variability in brightness and radial velocity with mass loss suggests a look at the past behavior of α Ori for evidence of events that may have signaled the ejection of substantial amounts of matter from the photosphere (Goldberg, 1984). Observations of visual brightness and radial velocity for this star have been carried out with varying degrees of regularity and accuracy for well over 60 years, the most accurate and homogeneous set of data having been acquired in 1917 through 1931 (Stebbins, 1931; Sanford, 1933). Although short-term changes in radial velocity and brightness were found to be uncorrelated in detail, Sanford (1933) noted one or two major disturbances in which decreasing velocity was accompanied by increasing light and vice versa.

The best example of such an event took place near the time of minimum radial velocity in the 6-year cycle, at about Julian day 2424500 (December 15, 1925). As shown in Figure 5-10, a large decrease in radial velocity after day 4500 was accompanied by an initial increase in brightness, followed by rapid fading. It is as though gaseous matter were ejected from the star, then diffused outward and condensed into grains which became optically thick at visible

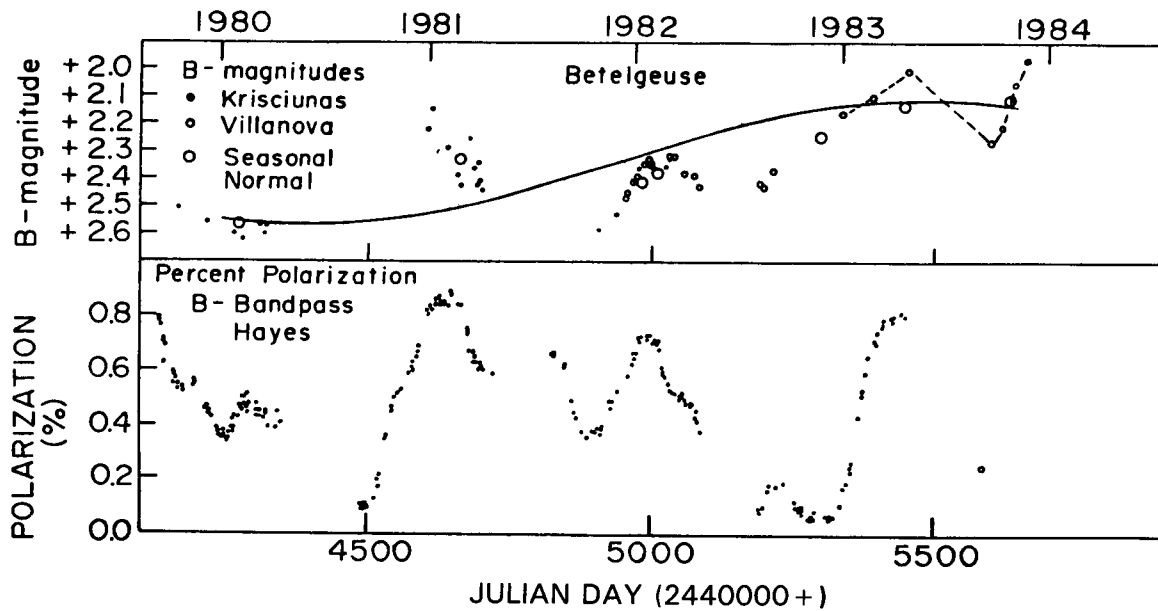


Figure 5-9. B-magnitudes and percent polarization of light from Betelgeuse. Large open circles are seasonal means, and solid curve is Stebbins' (1931) mean blue light curve (Guinan, 1983).

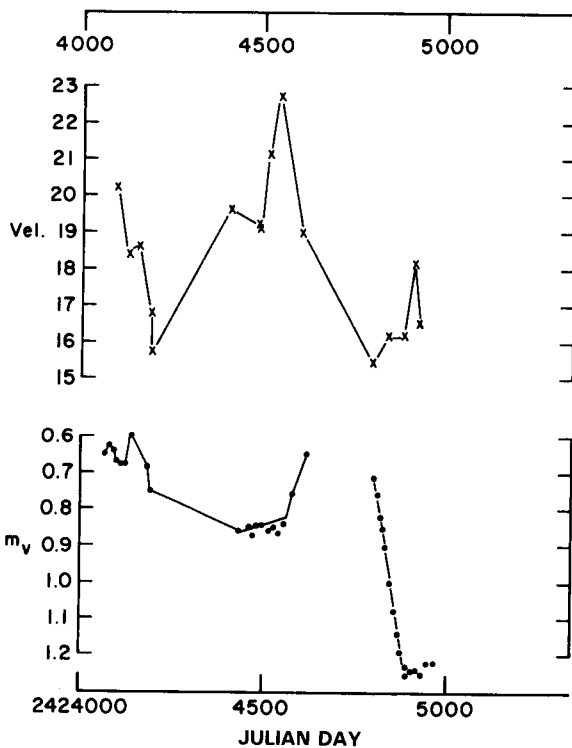


Figure 5-10. Light and velocity variations of α Ori around the time of the unusual event of December 15, 1925, when a period of decreasing radial velocity was followed by a steep decline in visual brightness (Goldberg, 1984).

wavelengths. Similar dust-forming episodes apparently occur during the development of slow novae of the DQ Herculis type (Gehrz et al., 1980) in which the visual extinction is accompanied by strongly enhanced infrared emission. Although photometric measures were not available, the records of the American Association of Variable Star Observers strongly suggest that in November 1944 (Adams, 1956) and again in 1978/1979 (Goldberg, 1979), similar events may have occurred at or soon after the minimum of the mean velocity curve.

At radial velocity minimum, a pulsating star has reached its maximum velocity of expansion and is beginning to decelerate. Given the enormous extension of a supergiant atmosphere, its motion probably lags that of the star, and the atmosphere will tend to continue accelerating outward past the minimum, as has been observed. At this time, instabilities in the atmosphere may trigger mass ejection, followed by the condensation of dust grains. In the future, systematic monitoring of α Ori with a variety of techniques before, during, and after the velocity minimum may clarify the relationship between the short-term brightness and velocity changes and the mass-loss process.

MECHANISMS

Any acceptable theory of mass-loss mechanisms must explain the location of stars showing high rates of mass loss on the HR diagram, as shown schematically in Figure 5-11. Roughly speaking, massive stellar winds, in the range 10^{-8} to $10^{-5} M_{\odot}/\text{yr}$ are found only among the more luminous stars lying in the upper half of the HR diagram. It is tempting to search for a single mechanism that can explain mass loss in both hot and cool stars, but this seems unlikely in view of the probable dependence of mechanisms on the environment. Thus, in the hot stars, the radiative force on atoms is optimized by the occurrence in the same wavelength region of both a strong radiation field and the resonance lines of abundant ions, whereas conditions in the low-temperature stars

are favorable for mass ejection by radiation pressure on dust grains. It also does not seem probable that the same mechanism can produce terminal velocities of 10 km/s in the cool stars and 3000 km/s in the hot stars. This section will be devoted to mechanisms that seem appropriate for the late-type giants, and the reader is referred to the monographs on B stars and on O, Of, and Wolf-Rayet stars for an account of hot-star mechanisms.

Figure 5-12, from a compilation by Reimers (1977b), shows the regions in the HR diagram in which late-type stars are found to have massive winds. All G and K supergiants, the later K giants, and all M giants and supergiants show circumstellar spectral lines. The region of the diagram containing stars with circumstellar dust shells is also shown, as are the locations of maser stars and long-period variables. IUE

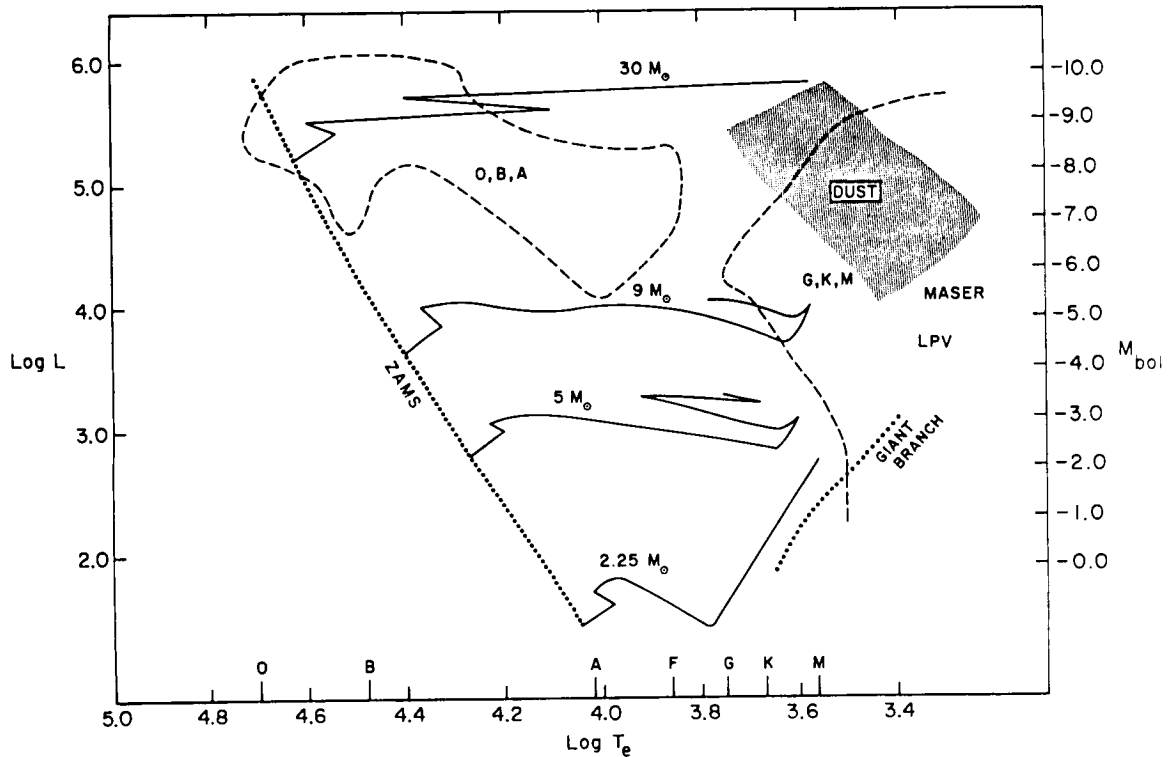


Figure 5-11. HR diagram in which dashed lines outline regions in which stars with high mass loss are found. Also shown are the zero-age main sequence (ZAMS), the giant branch, the locations of masers and long-period variables, evolutionary tracks, and the region occupied by stars showing the $10\text{-}\mu\text{m}$ dust signature (Goldberg, 1979).

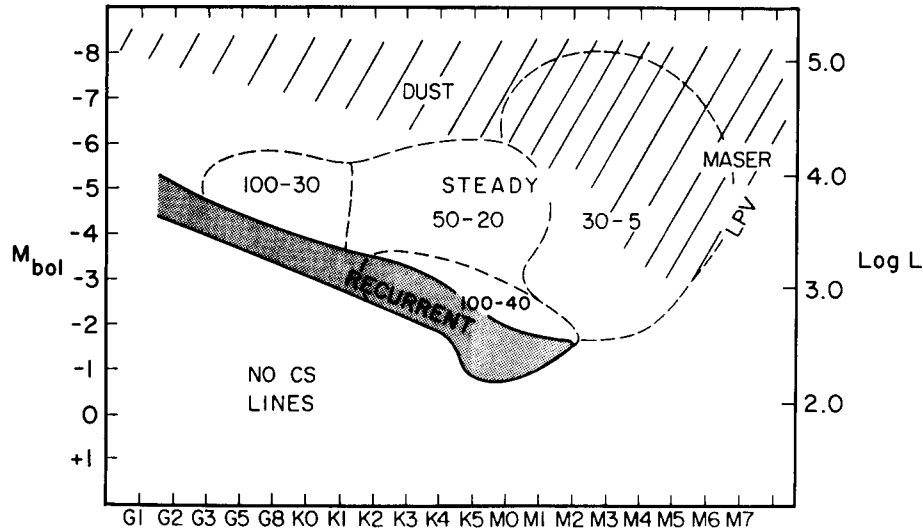


Figure 5-12. Portion of HR diagram for late-type stars, showing regions in which stars have expanding circumstellar shells. Approximate expansion velocities are shown, as well as the transition zone in which winds may be variable (Cassinelli, 1979).

and HEAO observations reveal that all late-type stars have chromospheres, but only stars with low mass loss have transition regions and high-temperature coronae (Linsky and Haisch, 1979; Vaiana et al., 1981). Linsky and Haisch (1979) first used IUE spectra to identify a boundary line in the HR diagram separating stars with coronae from those with only chromospheres.

Stars within the zone sometimes show both high-temperature lines such as C IV 1550 Å and CS lines, and the latter tend to show variability as well.

Similar boundaries, although not always coincident with one another, separate stars in which chromospheric expansion is indicated by the asymmetry of both the Ca II H and K emission (Stencel, 1978) and the Mg II h and k emission (Stencel and Mullan, 1980) and by stars with C IV line emission (Dupree, 1981) and X-ray emission (Vaiana et al., 1981). In reality, the boundary between stars with low and high mass loss is not a sharp line, but a relatively broad zone (Hartmann et al., 1980, 1981).

Some stars in the boundary zone are “hybrids,” so-called because their spectra show both displaced circumstellar lines and C IV line emission (Hartmann et al., 1980, 1981; Reimers, 1982). The CS lines in hybrid stars tend to show variability as well. On the average, terminal velocities increase from right to left, approaching 100 km/s near the boundary. The degree of sharpness of the boundary is still somewhat controversial (Haisch and Simon, 1982; Simon et al., 1982). The reason for the boundary is undoubtedly connected with evolutionary changes creating conditions favorable for high mass loss, but the nature of the changes is still not clear. On one side of the boundary, nonradiative energy beyond the chromosphere is dissipated into heat, and on the other side, the energy goes mainly into driving massive winds.

Several types of forces have been proposed to account for steady mass loss in red-giant stars, the principal ones being: (1) thermal gas pressure, (2) radiation pressure on dust grains, (3) shock waves, primarily those arising from pulsations in Mira stars, and (4) Alfvén waves. In addition, models of nonsteady or episodic

mass loss have been predicated on dynamical or pulsational instability, on convection, or on magnetic reconnection. Steady mass loss will be considered first.

Thermal Gas Pressure

Parker's original solar wind model has inspired numerous attempts to drive winds in late-type giants by thermal pressure, most recently by Hearn (1975), Mullan (1978), and Watanabe (1981). Basically, these models fail because the thermal energy inferred from the observed low wind temperatures is too low to overcome stellar gravity (Holzer et al., 1983). The observed mass-loss rates can be achieved only by postulating temperatures so high that the radiation emitted would far exceed that observed.

Radiation Pressure on Dust Grains

A complete theory of dust-driven mass loss should include consideration of matters such as grain formation (see Kwok, 1975; Deguchi, 1980; Draine, 1981; Lefèvre et al., 1982; Woodrow and Auman, 1982), the transfer of infrared continuum radiation (Jones and Merrill, 1976; Menietti and Fix, 1978; Rowan-Robinson, 1980), circumstellar shell chemistry (Goldreich and Scoville, 1976; Scalo and Slawsky, 1980; Huggins and Glassgold, 1982; Glassgold and Huggins, 1983 and this volume), and the dynamics of the gas and dust flow (Kwok, 1975; Goldreich and Scoville, 1976; Menietti and Fix, 1978; Tielens, 1983).

Calculations of the motion of gas in a circumstellar shell always assume a spherically symmetric atmosphere with steady flow governed by the equations of conservation of mass and momentum (Kwok, 1975):

$$\frac{d}{dr} (\rho \cdot v \cdot r^2) = 0, \quad (5-15)$$

$$\frac{d}{dr} \left(\frac{1}{2} v^2 \right) = - \left(\frac{1}{\rho} \right) \left(\frac{dP}{dr} \right) - \frac{GM_*}{r^2} [1 - \mathfrak{F}(r)], \quad (5-16)$$

where v is the flow velocity, ρ is the density, P is the gas pressure, M_* is the mass of the star, and $\mathfrak{F}(r)$ is the ratio of the radiative force to the gravitational force:

$$\mathfrak{F}(r) = \frac{\left(\frac{\pi a^2 \bar{Q} L n_{gr}}{4\pi c r^2} \right)}{\left(\frac{GM_* \rho}{r^2} \right)}, \quad (5-17)$$

where \bar{Q} is the flux weighted mean of the radiation pressure efficiency of the grains, n_{gr} is the number density of the grains, a is the grain radius, and L is the stellar luminosity.

These equations must be solved in conjunction with the equation of motion of the grains:

$$F_{rad} = \left(\frac{4}{3} \pi a^3 \rho_s \right) \frac{dv_{gr}}{dt} + \frac{GM_* (4/3 \pi a^3 \rho_s)}{r^2} + F_{drag}, \quad (5-18)$$

where v_{gr} is the velocity of the grain, ρ_s is its density, and F_{drag} is the drag force produced by collisions with gas molecules. It is easy to show that, for grain radii of about $0.1 \mu\text{m}$ in late-type giants, the gravitational force is much smaller than the radiative force and can therefore be neglected. It has also been found that, for α Ori for example, the terminal velocity is reached by grains in a distance on the order of one solar radius. Therefore,

$$F_{rad} = F_{drag}. \quad (5-19)$$

F_{drag} is usually approximated by (Kwok, 1975):

$$F_{drag} = \alpha \cdot \pi a^2 \cdot \rho v_d (v_T^2 + v_d^2)^{1/2}, \quad (5-20)$$

where ρ is the gas density, v_d is the drift velocity of the dust grains relative to the gas molecules, v_T is essentially the thermal velocity, and α is an elasticity factor assumed to be equal to $3/4$. At this point, additional equations

must be introduced according to whatever assumptions are made about the temperature distribution, the sites of grain formation, the fraction of gas in the form of grains, and their growth and sputtering rates.

The assumptions that are made often depend on the primary goals of the models. Thus, the models of Kwan and Hill (1977), Kwan and Linke (1982), and Morris (1980), which were described in the section *Millimeter Waves*, assumed a priori that the mass loss is driven by dust and were used to calculate molecular line emission, with the rate of mass loss as an adjustable parameter to be determined from observation. In this section, we shall be concerned with models whose purpose it is to test various aspects of the dust-driven mechanism.

Following the approximate analytical expressions derived by Gehrz and Woolf (1971), Kwok (1975) made the first numerical solutions of the equations of motion, taking account of radiation pressure on grains, stellar gravity, growth and sputtering of grains, and momentum transfer from grain to gas. Kwok believed that radiative heating and cooling could be neglected and assumed the adiabatic law for the temperature variation. In their investigation of the physical properties of OH/IR stars, Goldreich and Scoville (1976) showed that collisions between gas molecules and dust grains are a significant source of heating and that the gas is cooled both by adiabatic expansion and by H₂O molecular emission. The resulting temperature distribution is markedly different from the adiabatic law. Goldreich and Scoville also considered the chemical reactions that control the abundances of OH and H₂O.

Menietti and Fix (1978) solved the equation of motion of the gas in cool luminous stars, taking account of the radiative properties of both the gas and the dust. The density, temperature, and radiative energy distributions were not assumed in advance, but were derived from the modeling process. Similarly, Rowan-Robinson (1980) has developed accurate solutions to the equation of radiative transfer for the purpose of predicting the radiative energy distributions of stars throughout the wavelength region 0.4

to 30 μm . The model consists of a blackbody of given radius and temperature at the center of a spherically symmetric dust shell. The free parameters of the model are the temperature of the central star, the condensation temperature of the grains, which is also the temperature of the inner boundary of the shell, the limiting optical depth at short wavelengths through the shell, the density gradient in the shell, the ratio of the inner and outer radii of the shell, and the interstellar extinction. The parameters are determined by fitting model calculations to the observed spectra. Models have been derived and applied to the observed spectra of 156 late-type stars, including early M stars (Rowan-Robinson and Harris, 1982), stars of type M5 and later (Rowan-Robinson and Harris, 1983a), carbon stars (Rowan-Robinson and Harris, 1983b), and OH/IR stars showing double shells (Rowan-Robinson, 1982).

The model by Deguchi (1980), of the flow in O-rich stars, focuses mainly on the process of grain formation. The theory of grain nucleation is used to calculate the number density of grains, the grain sizes, and the final amount of metals remaining in gaseous form. Woodrow and Auman (1982) construct time-dependent models of carbon-rich red giants, making use of the equations of hydrodynamics, the theory of grain nucleation and growth, and the equations describing a gray model atmosphere in LTE and radiative equilibrium.

The most recent model of dust-driven gas flow in O-rich Mira stars (Tielens, 1983) is also the most detailed and complete. The starting point of the model is the observational evidence (Hinkle, et al., 1982) that the outward motion of the pulsating photospheres of Miras generates shock waves that elevate matter to a stationary layer about 5 stellar radii above the photosphere, where the temperature is less than 1000 degrees and therefore low enough to permit dust grains to condense. The stationary layer is, in effect, a reservoir for the matter in the wind.

Some general conclusions can be drawn from these modeling investigations. Circumstellar gas shells in late-type giants and

supergiants are heated by stellar radiation and by grain/gas collisions. At least in the late-M Miras and supergiants, the gas is heated by the drag force and cooled by H₂O emission and adiabatic expansion (Goldreich and Scoville, 1976). The velocity gradient also plays an important part in the determination of the temperature structure (Tielens, 1983). When the density is high enough, photon trapping can slow radiative cooling in the absence of a velocity gradient. Thus, the temperature structure of the gas is coupled to the dynamics of the outflow.

Observed radiative energy distributions are consistent with an r^{-2} law for the density distribution (Rowan-Robinson and Harris, 1982, 1983a, 1983b). However, detailed modeling of the flow (Menietti and Fix, 1978; Tielens, 1983) shows that the density falls off much more rapidly than as r^{-2} until after the sonic point is reached. Correspondingly, in Tielens' model, the velocities increase rapidly from the stationary layer, at distance r_1 , to a terminal value at about $10 r_1$. An example given by Tielens (1983) shows that, if the mass-loss rate is calculated from the total mass column density by Equation (5-3) on the assumption that the velocity is constant, the rate will be overestimated by a factor of 3 to 4.

The model calculations also demonstrate that it is difficult to produce 10- μ m excesses in O-rich stars with clean silicates (Jones and Merrill, 1976; Menietti and Fix, 1978; Rowan-Robinson and Harris, 1982, 1983a). In the carbon stars, amorphous carbon grains with absorption efficiency proportional to frequency give better agreement between observed and calculated energy distributions than does graphite (Rowan-Robinson and Harris, 1983b). Empirical values of the optical depth of the silicate feature at 10 μ m, derived from comparison of model calculations with observation, are strongly model-dependent. For example, the values derived by Rowan-Robinson and Harris (1982, 1983a) are smaller than those of Hagen (1978), in some cases by a factor of 20 and in others by a factor of about 200.

Differences in assumed grain parameters can account for a factor of 20, whereas another factor of 10 may occur in stars for which the use of an optically thin model (Hagen, 1978) may not have been justified. Until these disagreements can be resolved, it is premature to draw conclusions from dust column densities inferred from the 10- μ m optical depth (Hagen, 1978; Hagen et al., 1983; Bernat, 1981).

The fraction of metals remaining in the gaseous state varies with the mass-loss rate (Deguchi, 1980) from 1 to 10 percent for $\dot{M} = 10^{-5} M_{\odot}/\text{yr}$, and <1 percent for $\dot{M} < 3 \times 10^{-6} M_{\odot}/\text{yr}$. Owing to the large drift velocity of the grains relative to the gas, the dust-to-gas ratio is not a constant with distance (Tielens, 1983). This is important in the estimation of mass-loss rates from the 10- μ m feature.

We come finally to the most important question. Does radiation pressure on dust grains drive the observed mass flows in late-type giants and supergiants? The most important parameters on which the success of the mechanism depends (Kwok, 1975; Menietti and Fix, 1978) are the stellar luminosity, L , the mass, M_* , which together determine the distance of the sonic point, the effective temperature, T_{eff} , and the most critical factor, the density of gas at the condensation point, ρ_c , which must be large enough both to ensure momentum coupling and to hold down the sputtering rate by keeping the drift velocity low. The condensation-point gas density is a function of both effective temperature, T_{eff} , which controls the distance of the condensation point from the star, and the scale height, which depends on the stellar mass, or luminosity, L . Kwok (1975) has calculated the minimum density at the condensation point required for mass ejection from stars of various luminosities and effective temperatures, and has shown that the more luminous the star, the lower the temperature at which mass loss is possible. Figure 5-13 is a plot of $\log L$ versus T_{max} , the maximum effective temperature for which dust-driven mass loss can occur. Also plotted are the positions in the diagram of four red supergiants, α Ori, α Sco,

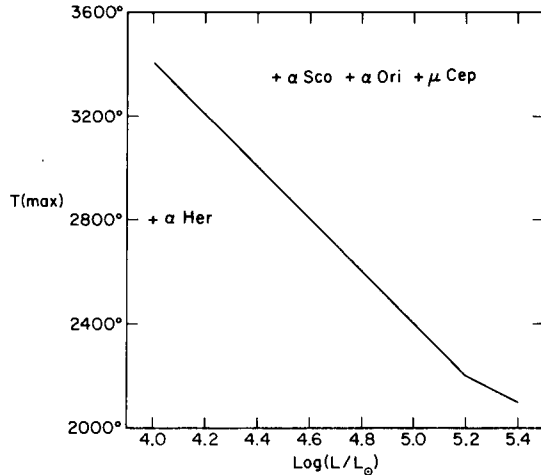


Figure 5-13. The maximum effective temperature at which dust-driven mass loss would be expected to occur, as a function of stellar luminosity according to model calculations by Kwok (1975). The positions of the four supergiants, α Ori, α Sco, α Her, and μ Cep, are indicated by crosses.

α Her, and μ Cep. Only for α Her is the temperature low enough to allow condensation at high enough gas densities. These calculations are not necessarily fatal to the dust-driven hypothesis for the hotter stars (Draine, 1981). For example, the gas density may be increased by clumping or by the ejection of discrete clouds, and "clean" grains can form relatively close to the star and gather up impurities as they move away. Note also that in α Ori, and probably in other red giants as well, the photosphere is greatly distended, its scale height being on the order of a stellar radius (Balega et al., 1982). Calculations based on plane-parallel model atmospheres give erroneously high temperatures for spherically extended atmospheres (Schmid-Burgk and Scholz, 1981). It remains to be investigated whether the temperatures are lowered sufficiently in the higher density regions to allow grain formation.

An empirical test of the dust mechanism can be made by comparing observed rates of mass loss with rates estimated on the assumption that the total energy radiated by grains in the infrared equals the energy absorbed in imparting

momentum to the grains (Knapp et al., 1982). The rate of grain-driven mass loss is related to the infrared flux at the Earth by

$$M V_0 / D^2 = \beta F / c, \quad (5-21)$$

where β is a factor measuring the amount of dust in the envelope, D is the distance to the star, V_0 is the terminal velocity, and F is the bolometric flux measured at the Earth, derived by integrating the continuum spectrum inferred from published IR fluxes. On the premise that the dust mechanism works for the oxygen stars, Knapp et al. (1982) calculate β from Equation (5-21) and find it to be correlated with the color ($3.5 \mu\text{m}$) - ($11 \mu\text{m}$), which is known to measure the dust content of circumstellar envelopes. The correlation may be the best evidence to date that the dust mechanism is responsible for mass loss in the cooler O-rich stars. It is still not clear whether or not the dust mechanism is adequate to drive the mass loss in the carbon stars or whether some additional mechanism needs to be invoked.

Shock Waves

The conclusion from both theoretical and observational considerations is that radiation pressure on dust grains can drive mass loss at the observed rates in late M and S giants and supergiants, but that some additional force or forces are needed in the early M-types and especially in the carbon stars. In addition to radiation pressure on grains and thermal pressure, wave pressure has received considerable attention as an important source of momentum and energy in late-type stars, either from shock waves generated by pulsation in Mira stars (Willson and Hill, 1979; Willson, 1981; Wood, 1979, 1981) or from Alfvén waves (Hartmann and McGregor, 1980, 1982; Hartmann and Averett, 1984). Calculations of the dynamic response of model Mira atmospheres to a series of periodic shocks driven by an oscillating piston have shown that high rates of mass loss are possible in such models. Two extreme

cases have been studied. Both Willson and Hill (1979) and Wood (1979) found that isothermal shock models showed very low rates of mass loss, about $10^{-12} M_{\odot}/\text{yr}$, whereas in the adiabatic limit, the shocks give unrealistically high rates, about $10^{-2} M_{\odot}/\text{yr}$, and unacceptably large values of the terminal velocity. Thus, the critical point in the theory is whether the shocks generated by pulsation are isothermal or adiabatic. Some compromises are possible:

1. Periodic isothermal shocks can levitate the atmosphere and thereby increase grain-driven mass loss by a factor of about 40, according to Wood (1979). Another estimate by Jones et al. (1981) is that the increase in atmospheric scale height by pulsation can enhance the rate of grain-driven mass loss by several orders of magnitude.
2. In the lower atmosphere, where the emission lines originate, the shocks may be isothermal, but higher up, as the density falls, the rates of cooling diminish and the shocks may become adiabatic (Willson and Hill, 1979).

Alfvén Waves

Hartmann and McGregor (1980, 1982) have studied the response of model atmospheres of red giants and supergiants to the passage of Alfvén waves of about solar magnitude, with stellar gravity as the main parameter. They conclude that the force due to Alfvén waves can account for observed mass-loss rates and terminal velocities, provided that the waves are dissipated over a distance of the order of a stellar radius by damping arising from collisions between ions and neutral atoms. The theory is an attractive one, both because a single parameter—stellar gravity—controls the rate of mass loss and because it predicts that red giants have extended warm chromospheres as observed. However, a detailed study of Alfvén waves in stellar atmospheres (Holzer et al.,

1983) concludes that cool winds driven by Alfvén waves will not exhibit both high mass loss and low terminal velocity. The basic problem with this and other stellar wind mechanisms, as Holzer et al. (1983) point out, is that energy inserted into the flow in the subsonic region increases the mass flux but not the velocity, whereas in the supersonic region, the addition of energy increases the terminal speed without affecting the mass loss. Thus, the mechanism must be such that a large fraction of the energy is dissipated in the subsonic flow region, with just the right small amount left over for the supersonic flow to overcome gravity and yet limit the terminal velocity to the observed fraction of the velocity of escape from the photosphere.

Recently, Hartmann and Averett (1984) have applied the theory to construct a model of the extended chromosphere of α Ori. Assuming that a wind of about $10^{-6} M_{\odot}/\text{yr}$ is driven by dissipating Alfvén waves, they reproduce the observed free-free emission at radio wavelengths, the $H\alpha$ emission observed by speckle interferometry, and the emission fluxes in a number of spectral lines. However, the model fails to reproduce the observed shapes of chromospheric line profiles, which suggests that, although the waves can heat and extend the chromosphere, the observed chromospheric expansion velocities are three times smaller than those predicted by the model. Hartmann and Averett (1984) suggest two possible ways out of this problem. Either the waves simply distend the atmosphere so that the gas density at the grain condensation point is high enough to maintain dust-driven mass loss, or spatial and temporal time variability in wave generation and damping may lead to composite emission from low- and high-velocity ejections.

If massive winds in late-type stars are driven by Alfvén waves, the stars should have extended chromospheres, which emit microwave radiation at centimeter wavelengths. Such radiation has been detected from several K and early M giants and supergiants (Drake and Linsky, 1984), but its weakness or absence in 31

evolved red giants surveyed by Spergel et al. (1983) argues against the effectiveness of the Alfvén-wave mechanism in the late M stars.

Mechanisms for Nonsteady Mass Loss

A number of mechanisms have been proposed for sporadic or nonsteady mass loss in red giants. Schwarzschild (1975) suggested that large-scale convection might trigger the ejection of a massive cloud by some process as yet unknown. Such ejections might cause both the irregular brightness variations observed in cool variable stars and the observed ordered changes in the linear polarization. Bloemhof et al. (1984) suggest that such localized and temporary phenomena are consistent with the observed asymmetric distribution of dust around α Ori. Wood (1979) has proposed that isothermal shock waves in the atmosphere of a Mira star generate mass loss by levitating the atmosphere to heights at which grains condense. Jones et al. (1981) have shown that the mass-loss rate may be enhanced by several orders of magnitude, as compared with grain-driven mass loss alone. We have already referred to the evidence that such a process may be at work in χ Cygni and in other Miras as well (Hinkle et al., 1982). In stars like α Ori, matter might be transported to the dust layer by shock waves associated with the irregular fluctuations in brightness, as suggested, for example, by Schwarzschild (1975) and by Kafatos and Michalitsianos (1979).

The region in α Ori between the photosphere and the base of the shell, which we tentatively identify as the chromosphere, may be the source of the Fe II emission lines observed by Boesgaard and Magnan (1975) and Boesgaard (1979) near 3100 Å, by van der Hucht et al. (1979) in the 2750 to 3165 Å region, and by Carpenter (1984) in the 2300 to 3000 Å region. Measurements of these lines have given conflicting results. Boesgaard and Magnan found that the motions derived from the Fe II lines were closely coupled to the photospheric motions, but indicated matter falling into the photosphere at an average speed of about

5 km/s. Conversely, van der Hucht et al.'s measurements from a balloon showed an average blue-shift of 14 km/s relative to the photosphere. From high-resolution IUE spectra, Carpenter (1984) found no evidence of strong coupling between photosphere and chromosphere and no systematic difference between the mean velocities of the photosphere and chromosphere. He interpreted the relation between line asymmetry and line strength as evidence for a schematic velocity field that is initially constant with height and then increases outward to a maximum value before decreasing to an asymptotic value. These apparently contradictory results might be resolved if the velocity fields varied with time, which might be expected if the Fe II emission is responsive to fluctuations in photospheric activity. On the other hand, Carpenter's data are more complete and of higher quality than those obtained from the ground and with balloons. Continued monitoring from IUE would be very important in resolving this question.

Burke (1972) suggested that rising shock waves ejecting matter would be expected whenever there is pulsation or a strong convection zone near the surface of a star. The mass would be ejected preferentially from the equator in the direction of rotation and would lead to loss of angular momentum without the need for magnetic fields. Kafatos and Michalitsianos (1979) have applied this mechanism to the determination of the rate of spin-down of red supergiants. The ejection of matter is predicted to form a disk or torus of silicate grains in the equatorial regions.

Mass loss is also predicted to occur from dynamically and pulsationally unstable envelopes of red-giant stars (Tuchman et al., 1978, 1979, and earlier references therein). According to Tuchman et al. (1978), dynamical instability sets in when, owing to partial ionization and/or partial dissociation, the quantity, γ , the adiabatic value of the logarithmic pressure gradient, falls below 4/3 over a sufficiently large and/or deep region. An initial expansion turns into violent oscillations in the envelope. Shocks

generated within the envelope lead to repetitive episodes of mass loss on a time scale of < 30 years, which would cause large amounts of mass to be lost during evolutionary time scales. Newer calculations by Fox and Wood (1982) show that the apparent instabilities are caused by the neglect of nonadiabatic effects in the models.

Magnetic Reconnection

A few years ago, Mullan (1978) suggested that the boundary in the HR diagram between stars with high and low mass loss is a supersonic transition locus (STL), along which the sonic points of the wind dip below the heights reached by the tops of spicules. Holzer (1980) and others have shown the STL hypothesis to be untenable, and Mullan (1982) has proposed instead that the boundary is caused by a transition in magnetic topology. (See also Mullan and Ahmad, 1982; Mullan and Steinolfson, 1983). The idea is that, since X-ray emission in the Sun is associated with closed magnetic loops and the solar wind is enhanced over coronal holes where the field is mainly open, massive winds and the absence of X rays may result when stars are unable to maintain closed magnetic field lines in the steady state. With the aid of Pneuman's (1968) model of helmet streamers, Mullan (1982) investigates the question of where in the HR diagram the transition from closed to open field configurations might occur. Pneuman (1968) found that helmet streamers would be unstable and would not exist in a steady state when the parameter,

$$\Psi = \mu \cdot G \cdot M_* \cdot m_p / R_* kT \quad , \quad (5-22)$$

is smaller than 4. In Equation (5-22), μ is the mean molecular weight, m_p is the proton mass, M_* and R_* are the mass and radius of the star, respectively, and T is the temperature at the sonic point. Since the radius, R_s , of the sonic point is $\mu GM_* m_p / 2 kT$, the condition that long-lived closed lines can exist is $R_s > 2 R_*$. The locus $R_s = 2 R_*$ on the HR diagram defines a so-called magnetic topology transition

locus (MTTL) which happens to closely follow the boundary between stars with weak and strong mass loss. Once it is accepted that the onset of massive winds in red giants is associated with open field lines, the Alfvén-wave mechanism may be invoked to drive the wind. Alternatively, Mullan (1981) has speculated that after unstable emerging loops are ejected from the surface, field-line reconnection at the base of the loops furnishes the energy for accelerating them upward.

EVOLUTIONARY CONSEQUENCES OF MASS LOSS

Supernovae

The evolutionary effects of mass loss on red giants have been well reviewed, for example, by Iben (1981b) and Renzini (1981a, 1981b). The most convincing evidence comes from supernovae. In the absence of mass loss, all stars with initial masses less than $1.44 M_\odot$ would become white dwarfs, whereas all those with larger masses would explode as supernovae of either Type I or Type II, depending on the mass. It is estimated that, without mass loss, the frequency of supernovae in a galaxy would be one per year, which is about 10 times greater than observed. Observed rates of mass loss allow one to predict that stars with initial masses as large as 5 to $8 M_\odot$ can end up as white dwarfs. The predicted frequency of supernovae is reduced to about the observed level.

Stars in Globular Clusters

A second theoretical argument for mass loss in red giants is morphological and is based on the observed distribution of stars on the giant and horizontal branches of Population II globular clusters. Evolutionary calculations without mass loss give perfect fits to the main-sequence and red-giant branches of the HR diagram, but the tip of the asymptotic giant branch (AGB) is about 2.5 mag too bright and the horizontal branch (HB) is too short: blue

stars and RR Lyrae stars are absent. Stars embarking on the red-giant branch (RGB) are estimated to have initial masses of 0.8 to 0.9 M_{\odot} . The HB discrepancy may be removed if stars lose 0.2 M_{\odot} solar masses during the RGB phase before helium flash, whereas the AGB problem is resolved if an additional 0.1 M_{\odot} is lost during the AGB phase. The computed HB tracks are still too short, unless it is assumed that stars arriving at the HB have a spread in their masses of about 10 percent.

Evolutionary calculations incorporating mass loss as given by the revised Reimers formula, Equation (5-4), reproduce the observed morphology of the RGB, HB, and AGB in Population II globular clusters. It is claimed further that such morphological considerations put narrow constraints of about 10 percent on the correct values of mass-loss rates themselves. Judgment on this point must be reserved until more is known about the interior physics of stars (e.g., convection, neutrino physics, turbulent diffusion, primordial chemical composition, and meridional mixing).

Composition of Interstellar Matter

The theory of stellar evolution also predicts that red supergiants may be the most important source of interstellar grains, both from mass loss and from supernova explosions. Variations in the surface composition during the AGB phase should affect grain characteristics in the winds. At the beginning of the AGB phase, the star is type M with C/O < 1, and consequently, silicate grains can form in the wind. Later, the star becomes a carbon star with C/O > 1; after the third dredge-up (Iben, 1981a), O is locked up in CO, but there is an abundance of free carbon and C-rich molecules. Hence, grains in the winds will contain not silicates but ample quantities of C-rich particles such as amorphous carbon grains, graphite, and SiC grains.

Formation of Planetary Nebulae

The formation of planetary nebulae is one of the most spectacular consequences of mass

loss from red giants, and in fact, observations of planetary nebulae are providing critical tests of the entire theory of the late stages of stellar evolution, in which mass loss plays a critical role. It is generally accepted that planetary nebulae are produced by asymptotic branch stars, which eject their hydrogen-rich envelopes, after which the stellar remnant evolves to a high temperature and radiates the far-UV photons needed to excite the envelope. By what mass-loss process is the envelope ejected and at what rate? Assuming with Renzini (1981b) that a typical planetary nebula has a mass of 0.2 M_{\odot} , a radius of 0.1 pc, and an expansion velocity of 20 km/s, we find that the nebula must form in about 5000 years, which requires a mass-loss rate of about $4 \times 10^{-5} M_{\odot}/\text{yr}$. Since this rate is an order of magnitude greater than that given by the Reimers formula when applied near the top of the AGB, Renzini postulated the more or less sudden onset of a "superwind" that would turn on at the end of the AGB phase and operate for a relatively short time.

Such a superwind could take one of several forms. It could occur when Mira variables switch oscillation modes from the first overtone to the fundamental (Wood, 1974, 1981; Tuchman et al., 1979; Fox and Wood, 1982) or by the onset of pulsation in Miras, which Willson (1981) believes is normally in the fundamental mode. It was once believed that the formation of planetary nebulae might be caused by dynamical instability, but detailed calculations (Tuchman et al., 1978) have shown that the relevant models should stabilize while the envelope mass is still too large (> 0.1 M_{\odot}). The mode-switching mechanism leads to a relatively sudden ejection of the stellar envelope in less than 1000 years (Tuchman et al., 1979). A different scenario which does not require sudden ejection has been proposed by Kwok et al. (1978) and has been elaborated by Kwok (1982). The steady mass loss eventually depletes the H-rich envelope, exposing the hot core and causing a sudden change in the mass-loss mechanism to one of radiation pressure on ions. The velocity of the wind increases by a factor of 100, and the snowplow effect builds up a dense

shell at the interface between the new and the old wind. In this model, the planetary nebula forms in about 3000 years. The distinction between steady and sudden ejection seems artificial, inasmuch as both mechanisms require a sudden increase in mass-loss rate, and the difference in time scales is well within the uncertainties of the calculations. Moreover, interaction is bound to occur between the old circumstellar shell and the new wind, no matter which mechanism is operative.

Recent observations of unidentified OH/IR stars (Baud et al., 1981; Engels et al., 1983) are providing considerable evidence in favor of Mira variables as progenitors of planetary nebulae, as was suggested by Wood and Cahn (1977). As stars evolve up the AGB, they lose mass steadily, and at some value of the luminosity, which depends on the mass, they begin pulsating as Mira variables in the first-overtone mode. As the luminosity increases, so do the radius and the period. Eventually, for a given stellar mass, a star reaches a value of the luminosity at which the fundamental mode becomes dominant, the envelope is ejected, and the planetary nebula forms in a matter of a few thousand years. The evolutionary model of Wood and Cahn (1977) was developed in considerable detail by Tuchman et al. (1979), but encountered several disagreements with observation, the most serious being the termination of first-overtone pulsation at much lower luminosities and shorter periods than observed, and the occurrence of dynamical instabilities at the point at which the fundamental mode takes over, which limits the observed periods to less than 600 days. It now appears that the instabilities do not in fact occur (Fox and Wood, 1982) and hence that pulsations with periods longer than 2000 days are stable.

From a study of the statistical properties of about 20 OH/IR stars, Baud and Habing (1983) were able to investigate the physical parameters that determine the OH luminosity. The OH luminosity is correlated with the size of the circumstellar shell and with the mass-loss rate. They make the basic assumption that the se-

quence of OH/IR stars arranged in order of increasing period and mass-loss rate (see Table 5-3) is an evolutionary sequence, and they derive a timescale of between 0.6×10^5 and 6.5×10^5 years for main-sequence masses between 0.7 to $6 M_{\odot}$ for the OH maser lifetime. Of this time, 99 percent is spent as a visible Mira with low mass loss, and 1 percent is spent as a luminous OH/IR star. Comparison of the derived physical parameters of the stars with the models of Fox and Wood (1982) suggests that the OH maser turns on at about the time that the pulsation mode switches from first overtone to fundamental. The models also predict that the longest periods go with the highest mass-loss rates, as found by Engels (1982). Engels et al. (1983) also conclude that OH/IR stars are AGB variables, but that they are probably in the same evolutionary stage as Miras. They argue that, since OH/IR stars show higher concentration to the galactic plane than Miras, they must have higher masses, in the range 2 to $10 M_{\odot}$. The high galactic concentration of unidentified OH/IR stars is not a problem (Baud and Habing, 1983), inasmuch as these stars represent only 1 percent of the OH/IR and are distant objects. It is less clear why there should be no low-mass OH/IR stars with high OH luminosity.

Radio continuum emission at 6 cm, which may be emitted by ionization fronts propagating into CS shells during the preplanetary nebula stage, has been detected in five of 32 cool evolved stars: NGC 7027, CRL 618, R Aqr, IRC + 10216, and O Ceti (Spergel et al., 1983). Model calculations predict that, in objects with low mass-loss rates, $M < 10^{-4} M_{\odot}/\text{yr}$, a planetary nebula is produced in $< 10^3$ years after the hot core is exposed. In those with intermediate masses, 4 to $6 M_{\odot}$, and high mass-loss rates, the ionization front moves so slowly that the shell is always ionization-bounded, and most of the mass is ejected as neutral gas and dust. NGC 7027 is an example of a recently formed planetary nebula, while CRL 618 is a protoplanetary nebula with its hot core still obscured by dust, and IRC + 10216

may or may not ever reach the planetary stage. Thus, the requirement for PN formation is a short period of very high mass loss, such as is found in long-period OH/IR sources, followed by one of reduced mass loss to allow the rapid propagation of an ionization front.

REFERENCES

- Adams, W.S. 1956, *Astrophys. J.*, **123**, 189.
- Adams, W.S., and MacCormack, E. 1935, *Astrophys. J.*, **81**, 119.
- Balega, Y., Blazit, A., Bonneau, D., Koechlin, L., Foy, R., and Labeyrie, A. 1982, *Astron. Astrophys.*, **115**, 253.
- Baud, B. 1981, *Astrophys. J. (Letters)*, **250**, L79.
- Baud, B., and Habing, H.J. 1983, *Astron. Astrophys.*, **127**, 73.
- Baud, B., Habing, H.J., Matthews, H.E., and Winnberg, A. 1979, *Astron. Astrophys. Supplement*, **35**, 179.
- Baud, B., Habing, H.J., Matthews, H.E., and Winnberg, A. 1981, *Astron. Astrophys.*, **95**, 156.
- Bernat, A.P. 1976, Thesis, University Microfilms International.
- Bernat, A.P. 1977, *Astrophys. J.*, **213**, 756.
- Bernat, A.P. 1981, *Astrophys. J.*, **246**, 184.
- Bernat, A.P. 1982, *Astrophys. J.*, **252**, 644.
- Bernat, A.P., Hall, D.N.B., and Ridgway, S.T. 1979, *Astrophys. J. (Letters)*, **233**, L135.
- Bloemhof, E.E., Townes, C.H., and Vanderwyck, A.H.B. 1984, *Astrophys. J. (Letters)*, **276**, L21.
- Boesgaard, A.M. 1979, *Astrophys. J.*, **232**, 485.
- Boesgaard, A.M., and Hagen, W. 1979, *Astrophys. J.*, **231**, 128.
- Boesgaard, A.M. and Magnan, C. 1975, *Astrophys. J.*, **198**, 369.
- Brooke, A.L., Lambert, D.L., and Barnes, T.G., III. 1974, *Pub. Astron. Soc. Pacific*, **86**, 419.
- Burke, J.A. 1972, *Mon. Not. Roy. Astr. Soc.*, **160**, 233.
- Cacciari, C., and Freeman, K.C. 1981, in *Physical Processes in Red Giants*, ed. I. Iben and A. Renzini (Dordrecht: Reidel), p. 311.
- Cacciari, C., and Freeman, K.C. 1983, *Astrophys. J.*, **268**, 185.
- Carpenter, K.G. 1984, *Astrophys. J.*, **285**, 181.
- Cassinelli, J.P. 1979, *Ann. Rev. Astron. Astrophys.*, **17**, 275.
- Chapman, R.D. 1981, *Astrophys. J.*, **248**, 1043.
- Che, A., Hempe, K., and Reimers, D. 1983, *Astron. Astrophys.*, **126**, 225.
- Che, A., and Reimers, D. 1983, *Astron. Astrophys.*, **127**, 227.
- Clarke, D., and Schwarz, H.E. 1984, *Astron. Astrophys.*, **132**, 375.
- Cohen, J.G. 1976, *Astrophys. J. (Letters)*, **203**, L127.
- Cohen, M. 1980, *Astrophys. J. (Letters)*, **238**, L81.
- Cohen, M., and Schmidt, G.D. 1982, *Astrophys. J.*, **259**, 693.

- Deguchi, S. 1980, *Astrophys. J.*, **236**, 567.
- Deutsch, A.J. 1956, *Astrophys. J.*, **123**, 210.
- Deutsch, A.J. 1960, in *Stars and Stellar Systems*, **VI**, ed. J.L. Greenstein (Chicago: Univ. Chicago Press), p. 453.
- Draine, B.T. 1981, in *Physical Processes in Red Giants*, ed. I. Iben and A. Renzini (Dordrecht: Reidel), p. 317.
- Drake, S.A., and Linsky, J.L. 1984, in *Proc. Third Cambridge Workshop on Cool Stars, Stellar Systems and the Sun*, ed. S.L. Baliunas and L. Hartmann (Berlin: Springer-Verlag), p. 350.
- Dupree, A.K. 1980, in *Highlights of Astronomy*, **5**, IAU Montreal, p. 263.
- Dupree, A.K. 1981, in *Proc. Second Cambridge Workshop on Cool Stars, Stellar Systems and the Sun*, ed. M.S. Giampapa and L. Golub, SAO Special Report 392, **II** p. 3.
- Dupree, A.K., Hartmann, L., and Avrett, E.H. 1984, *Astrophys. J. (Letters)*, **281**, L37.
- Dyck, H.M., and Simon, T. 1975, *Astrophys. J.*, **195**, 689.
- Dyck, H.M., Zuckerman, B., Leinert, Ch., and Beckwith, S. 1984, *Astrophys. J.*, **287**, 801.
- Elitzur, M. 1981, in *Physical Processes in Red Giants*, ed. I. Iben and A. Renzini (Dordrecht: Reidel), p. 363.
- Engels, D. 1982, *Thesis*, Bonn.
- Engels, D., Kreysa, E., Schultz, G.V., and Sherwood, W.A. 1983, *Astron. Astrophys.*, **124**, 123.
- Engels, D., Schultz, G.V., and Sherwood, W.A. 1981, in *Physical Processes in Red Giants*, ed. I. Iben and A. Renzini (Dordrecht: Reidel), p. 401.
- Fazio, G.G., McBreen, B., Stier, M.T., and Wright, E.L. 1980, *Astrophys. J. (Letters)*, **237** L39.
- Forrest, W.J., et al. 1978, *Astrophys. J.*, **219**, 114.
- Fox, M.W., and Wood, P.R. 1982, *Astrophys. J.*, **259**, 198.
- Fusi-Pecci, F., and Renzini, A. 1976, *Astron. Astrophys.*, **46**, 447.
- Gehrz, R.D., Grasdalen, G.L., Hackwell, J.A., and Ney, E.P. 1980, *Astrophys. J.*, **237**, 855.
- Gehrz, R.D., and Woolf, N.J. 1971, *Astrophys. J.*, **165**, 285.
- Gilman, R.C. 1969, *Astrophys. J. (Letters)*, **155**, L185.
- Gilman, R.C. 1972, *Astrophys. J.*, **178**, 423.
- Glassgold, A.E., and Huggins, P.J. 1983, *Mon. Not. Roy. Astr. Soc.*, **203**, 517.
- Goldberg, L. 1979, *Quart. J. Roy. Astr. Soc.*, **20**, 361.
- Goldberg, L. 1984, *Pub. Astron. Soc. Pacific*, **96**, 366.
- Goldberg, L., Hege, E.K., Hubbard, E.N., Strittmatter, P.A., and Cocke, W.J. 1981, in *Proc. Second Cambridge Workshop on Cool Stars, Stellar Systems and the Sun*, ed. M.S. Giampapa and L. Golub, SAO Special Report 392, p. 131.
- Goldberg, L., Ramsey, L., Testerman, L., and Carbon, D. 1975, *Astrophys. J.*, **199**, 427.
- Goldreich, P. 1980, see discussion of paper by Hall (1980).

- Goldreich, P., and Scoville, N.J. 1976, *Astrophys. J.*, **205**, 144.
- Guinan, E.F. 1983, in *Proc. Third Cambridge Workshop on Cool Stars, Stellar Systems and the Sun*, ed. S. Baliunas and L. Hartmann (Berlin: Springer-Verlag), p. 336.
- Hagen, W. 1978, *Astrophys. J. Supplement*, **38**, 1.
- Hagen, W. 1980, in *Proc. First Cambridge Workshop on Cool Stars, Stellar Systems and the Sun*, ed. A.K. Dupree, SAO Special Report 389, p. 143.
- Hagen, W., Stencel, R.E., and Dickinson, D.F. 1983, *Astrophys. J.*, **274**, 286.
- Haisch, B.M., and Simon, T. 1982, *Astrophys. J.*, **263**, 252.
- Hall, D.N.B. 1980, in *Proc. IAU Symp. 87, Interstellar Molecules* (Dordrecht: Reidel), p. 515.
- Hartmann, L. and Avrett, E.H. 1984, *Astrophys. J.*, **284**, 238.
- Hartmann, L., Dupree, A.K., and Raymond, J.C. 1980, *Astrophys. J. (Letters)*, **236**, L143.
- Hartmann, L., Dupree, A.K., and Raymond, J.C. 1981, *Astrophys. J.*, **246**, 193.
- Hartmann, L., and McGregor, K.B. 1980, *Astrophys. J.*, **242**, 260.
- Hartmann, L., and McGregor, K.B. 1982, *Astrophys. J.*, **257**, 264.
- Harvey, P.M., Bechis, K.P., Wilson, W.J., and Ball, J.A. 1974, *Astrophys. J. Supplement*, **27**, 331.
- Hayes, D.P. 1980, *Astrophys. J. (Letters)*, **241**, L165.
- Hayes, D.P. 1981, *Pub. Astron. Soc. Pacific*, **93**, 752.
- Hayes, D.P. 1984, *Astrophys. J. Supplement*, **55**, 179.
- Hearn, A.G. 1975, *Astron. Astrophys.*, **40**, 355.
- Hempe, K. 1982, *Astron. Astrophys.*, **115**, 133.
- Hinkle, K.H., Hall, D.N.B., and Ridgway, S.T. 1982, *Astrophys. J.*, **252**, 697.
- Hjellming, R.M., and Newell, R.T. 1983, *Astrophys. J.*, **275**, 702.
- Holzer, T.E. 1980, in *Proc. First Cambridge Workshop on Cool Stars, Stellar Systems and the Sun*, ed. A.K. Dupree, SAO Special Report 389, p. 153.
- Holzer, T.E., Flå, T., and Leer, E. 1983, *Astrophys. J.*, **275**, 808.
- Honeycutt, R.K., Bernat, A.P., Kephart, J.E., Gow, C.E., Sandford, M.T., II, and Lambert, D.L. 1980, *Astrophys. J.*, **239**, 565.
- Hoyle, F., and Wickramasinghe, N.C. 1962, *Mon. Not. Roy. Astr. Soc.*, **124**, 417.
- Huggins, P.J., and Glassgold, A.E. 1982, *Astrophys. J.*, **252**, 201.
- Iben, I. 1981a, in *Physical Processes in Red Giants*, ed. I. Iben and A. Renzini (Dordrecht: Reidel), p. 3.
- Iben, I. 1981b, in *Proc. IAU Colloq. 59, Effects of Mass Loss on Stellar Evolution*, ed. C. Chiosi and R. Stalio (Dordrecht: Reidel), p. 373.
- Jewell, P.R., Webber, J.C., and Snyder, L.E. 1980, *Astrophys. J. (Letters)*, **242**, L29.

- Jones, T.W., and Merrill, K.M. 1976, *Astrophys. J.*, **209**, 509.
- Jones, T.W., Ney, E.P., and Stein, W.A. 1981, *Astrophys. J.*, **250**, 324.
- Jura, M. 1983a, *Astrophys. J.*, **267**, 647.
- Jura, M. 1983b, *Astrophys. J.*, **275**, 683.
- Jura, M., and Morris, M. 1981, *Astrophys. J.*, **251**, 189.
- Kafatos, M., and Michalitsianos, A.G. 1979, *Astrophys. J. (Letters)*, **228**, L115.
- Knapp, G.R., and Bowers, P.F. 1983, *Astrophys. J.*, **266**, 701.
- Knapp, G.R., and Morris, M. 1985, *Astrophys. J.*, **292**, 640.
- Knapp, G.R., Phillips, T.G., and Huggins, P.J. 1980, *Astrophys. J. (Letters)*, **242**, L25.
- Knapp, G.R., Phillips, T.G., Leighton, R.B., Lo, K.Y., Wannier, P.G., Wooten, H.A., and Huggins, P.J. 1982, *Astrophys. J.*, **252**, 616.
- Krisciunas, K. 1982, *IAU Info. Bull. Var. Stars*, No. 2104.
- Krisciunas, K. 1983, *IAU Info. Bull. Var. Stars*, in press.
- Kudritzki, R.P., and Reimers, D. 1978, *Astron. Astrophys.*, **70**, 227.
- Kunasz, P.B., and Hummer, D.G. 1974, *Mon. Not. Roy. Astr. Soc.*, **166**, 57.
- Kwan, J., and Hill, F. 1977, *Astrophys. J.*, **215**, 781.
- Kwan, J., and Linke, R.A. 1982, *Astrophys. J.*, **254**, 587.
- Kwok, S. 1975, *Astrophys. J.*, **198**, 583.
- Kwok, S. 1982, *Astrophys. J.*, **258**, 280.
- Kwok, S., Purton, C.R., and FitzGerald, P.M. 1978, *Astrophys. J. (Letters)*, **219**, L125.
- Lambert, D.L., Hinkle, K.H., and Hall, D.N.B. 1981, *Astrophys. J.*, **248**, 638.
- Lefèvre, J., Bergeat, J., and Daniel, J.-Y. 1982, *Astron. Astrophys.*, **114**, 341.
- Linsky, J.L., and Haisch, B.M. 1979, *Astrophys. J. (Letters)*, **229**, L27.
- Lo, K.Y., and Bechis, K.P. 1977, *Astrophys. J. (Letters)*, **218**, L27.
- Mallia, E.A., and Pagel, B.E.J. 1978, *Mon. Not. Roy. Astr. Soc.*, **184**, 55P.
- Mariotti, J.M., Chelli, A., Foy, R., Lena, P., Sibille, F., and Tchountonov, G. 1983, *Astron. Astrophys.*, **120**, 237.
- Mauron, N., Fort, B., Querci, F., Dreux, M., Fauconnier, T., and Lamy, P.H. 1984, *Astron. Astrophys.*, **130**, 341.
- McCarthy, D.W., Howell, R.R., and Low, F.J. 1980, *Astrophys. J. (Letters)*, **235**, L27.
- Menietti, J.D., and Fix, J.D. 1978, *Astrophys. J.*, **224**, 961.
- Merrill, K.M. 1977, in *IAU Colloq. 42, The Interaction of Variable Stars With Their Environment*, ed. R. Kippenhahn, J. Rahe, W. Strohmeier (Bamberg: Reimis-Sternwarte), p. 46.
- Mitchell, R.M., and Robinson, G. 1980, *Mon. Not. Roy. Astr. Soc.*, **190**, 669.
- Morris, M. 1975, *Astrophys. J.*, **197**, 603.
- Morris, M. 1980, *Astrophys. J.*, **236**, 823.
- Morris, M., and Alcock, C. 1977, *Astrophys. J.*, **218**, 687.

- Morris, M., Redman, R.O., Reid, M.J., and Dickinson, D.F. 1979, *Astrophys. J.*, **229**, 257.
- Mullan, D.J. 1978, *Astrophys. J.*, **226**, 151.
- Mullan, D.J. 1981, in *Physical Processes in Red Giants*, ed. I. Iben and A. Renzini (Dordrecht: Reidel), p. 355.
- Mullan, D.J. 1982, *Astron. Astrophys.*, **108**, 279.
- Mullan, D.J., and Ahmad, I.A. 1982, *Solar Phys.*, **75**, 347.
- Mullan, D.J., and Steinolfson, R.S. 1983, *Astrophys. J.*, **266**, 823.
- Newell, R.T., and Hjellming, R.M. 1982, *Astrophys. J. (Letters)*, **263**, L85.
- Peterson, R.C. 1981, *Astrophys. J. (Letters)*, **248**, L31.
- Peterson, R.C. 1982, *Astrophys. J.*, **258**, 499.
- Pneuman, G.W. 1968, *Solar Phys.*, **3**, 578.
- Pottasch, S.R. 1984, *Planetary Nebulae* (Dordrecht: Reidel).
- Reimers, D. 1975a, *Mém. Soc. Roy. Sci. Liège*, 6th Ser. **8**, 369.
- Reimers, D. 1975b, in *Problems in Stellar Atmospheres and Envelopes*, ed. B. Baschek, W.H. Kegel, and G. Traving (Berlin-Heidelberg, New York: Springer-Verlag), p. 229.
- Reimers, D. 1977a, *Astron. Astrophys.*, **61**, 217. (*Erratum* **67**, 161.)
- Reimers, D. 1977b, in *Proc. IAU Colloq. 42, The Interaction of Variable Stars with Their Environment*, ed. R. Kippenhahn, J. Rahe, W. Strohmeier (Bamberg: Remeis-Sternwarte).
- Reimers, D. 1981, in *Physical Processes in Red Giants*, ed. I. Iben and A. Renzini (Dordrecht: Reidel), p. 269.
- Reimers, D. 1982, *Astron. Astrophys.*, **107**, 292.
- Reimers, D., and Schröder, K.-P. 1983, *Astron. Astrophys.*, **124**, 241.
- Renzini, A. 1977, in *Advanced Stages in Stellar Evolution*, ed. P. Bouvier and A. Maeder (Geneva), p. 149.
- Renzini, A. 1981a, in *Proc. IAU Colloq. 59, Effects of Mass Loss on Stellar Evolution*, ed. C. Chiosi and R. Stalio (Dordrecht: Reidel), p. 319.
- Renzini, A. 1981b, in *Physical Processes in Red Giants*, ed. I. Iben and A. Renzini (Dordrecht: Reidel), p. 269.
- Ricort, G., Aime, A., Vernin, J., and Kadiri, S. 1981, *Astron. Astrophys.*, **99**, 232.
- Ridgway, S.T. 1981, in *Physical Processes in Red Giants*, ed. I. Iben and A. Renzini (Dordrecht: Reidel), p. 305.
- Roddier, C., and Roddier, F. 1983, *Astrophys. J. (Letters)*, **270**, L23.
- Rowan-Robinson, M. 1980, *Astrophys. J. Supplement*, **44**, 403.
- Rowan-Robinson, M. 1982, *Mon. Not. Roy. Astr. Soc.*, **201**, 281.
- Rowan-Robinson, M., and Harris, S. 1982, *Mon. Not. Roy. Astr. Soc.*, **200**, 197.
- Rowan-Robinson, M., and Harris, S. 1983a, *Mon. Not. Roy. Astr. Soc.*, **202**, 767.
- Rowan-Robinson, M., and Harris, S. 1983b, *Mon. Not. Roy. Astr. Soc.*, **202**, 797.

- Salpeter, E.E. 1974, *Astrophys. J.*, **193**, 585.
- Sanford, R.F. 1933, *Astrophys. J.*, **77**, 110.
- Sanner, F. 1976, *Astrophys. J. Supplement*, **32**, 115.
- Scalo, J.M., and Slawsky, O.B. 1980, *Astrophys. J. (Letters)*, **239**, L73.
- Schmid-Burgk, J., and Scholz, M. 1981, in *Physical Processes in Red Giants*, ed. I. Iben and A. Renzini (Dordrecht: Reidel), p. 341.
- Schwarz, H.E., and Clarke, D. 1984, *Astron. Astrophys.*, **132**, 370.
- Schwarzschild, M. 1975, *Astrophys. J.*, **195**, 137.
- Shawl, S.J. 1975, *Astron. J.*, **80**, 602.
- Simon, T., Linsky, J.L., and Stencel, R.E. 1982, *Astrophys. J.*, **257**, 225.
- Sopka, R.J., Hildebrand, R., Jaffe, D.T., Gatley, I., Roellig, T., Werner, M., Jura, M., and Zuckerman, B. 1985, *Astrophys. J. (Letters)*, **294**, 242.
- Spergel, D.N., Giuliani, J.L., Jr., and Knapp, G.R. 1983, *Astrophys. J.*, **275**, 330.
- Stebbins, J. 1931, *Pub. Washburn Obs., Univ. of Wisc.*, **15**, 177.
- Stencel, R.E. 1978, *Astrophys. J. (Letters)*, **223**, L37.
- Stencel, R.E., Kondo, Y., Bernat, A.P., and MacCluskey, G.E. 1979, *Astrophys. J.*, **233**, 621.
- Stencel, R.E., and Mullan, D.J. 1980, *Astrophys. J.*, **238**, 221; **240**, 718.
- Sutton, E.C., Betz, A.L., Storey, J.W.V., and Spears, D.L. 1979, *Astrophys. J. (Letters)*, **230**, L105.
- Sweigart, A.V., and Gross, P.G. 1978, *Astrophys. J. Supplement*, **36**, 405.
- Tielens, A.G.G.M. 1983, *Astrophys. J.*, **271**, 702.
- Tinbergen, J., Greenberg, J.M., and de Jager, C. 1981, *Astron. Astrophys.*, **95**, 215.
- Tuchman, Y., Sack, N., and Barkat, Z. 1978, *Astrophys. J.*, **219**, 183.
- Tuchman, Y., Sack, N., and Barkat, Z. 1979, *Astrophys. J.*, **234**, 217.
- Vaiana, G.S., et al. 1981, *Astrophys. J.*, **245**, 163.
- van der Hucht, K.A., Bernat, A.P., and Kondo, Y. 1980, *Astron. Astrophys.*, **82**, 14.
- van der Hucht, K.A., Stencel, R.E., Haisch, B.M., and Kondo, Y. 1979 *Astron. Astrophys.*, **36**, 377.
- Watanabe, T. 1981, *Pub. Astr. Soc. Japan*, **33**, 679.
- Werner, M.W., Beckwith, S., Gatley, I., Sellgren, K., Berriman, G., and Whiting, D.L. 1980, *Astrophys. J.*, **239**, 540.
- Weymann, R.J. 1962a, *Astrophys. J.*, **136**, 844.
- Weymann, R.J. 1962b, *Astrophys. J.*, **136**, 476.
- Willson, L.A. 1981, in *Physical Processes in Red Giants*, ed. I. Iben and A. Renzini (Dordrecht: Reidel), p. 225.
- Willson, L.A., and Hill, S.J. 1979, *Astrophys. J.*, **228**, 854.
- Wood, P.R. 1974, *Astrophys. J.*, **190**, 609.
- Wood, P.R. 1979, *Astrophys. J.*, **227**, 220.

Wood, P.R. 1981, in *Physical Processes in Red Giants*, ed. I. Iben and A. Renzini (Dordrecht: Reidel), p. 205.

Wood, P.R., and Cahn, J.H. 1977, *Astrophys. J.*, **211**, 499.

Woodrow, J.E.J., and Auman, J.R. 1982, *Astrophys. J.*, **257**, 247.

Woolf, N.J., and Ney, E.P. 1969, *Astrophys. J. (Letters)*, **155**, L181.

Zuckerman, B., Palmer, P., Gilra, D.P., Turner, B.E., and Morris, M. 1978, *Astrophys. J. (Letters)*, **220**, L53.

Zuckerman, B., Palmer, P., Morris, M., Turner, B.E., Gilra, D.P., Bowers, P.F., and Gilmore, W.S. 1977, *Astrophys. J. (Letters)*, **211**, L79.